# New CC0$\pi$ GENIE model tune for MicroBooNE

P. Abratenko,[33] R. An,[14] J. Anthony,[4] L. Arellano,[18] J. Asaadi,[32] A. Ashkenazi,[30] S. Balasubramanian,[11] B. Baller,[11] C. Barnes,[20] G. Barr,[23] V. Basque,[18] L. Bathe-Peters,[13] O. Benevides Rodrigues,[29] S. Berkman,[11] A. Bhanderi,[18] A. Bhat,[29] M. Bishai,[2] A. Blake,[16] J. Y. Book,[13] L. Camilleri,[9] D. Caratelli,[11] I. Caro Terrazas,[8] F. Cavanna,[11] G. Cerati,[11] Y. Chen,[1] D. Cianci,[9] J. M. Conrad,[19] M. Convery,[26] L. Cooper-Troendle,[36] J. I. Crespo-Anadón,[5] M. Del Tutto,[11] S. R. Dennis,[4] P. Detje,[4] A. Devitt,[16] R. Diurba,[21] R. Dorrill,[14] K. Duffy,[11] S. Dytman,[24] B. Eberly,[28] A. Ereditato,[1] J. J. Evans,[18] R. Fine,[17] G. A. Fiorentini Aguirre,[27] R. S. Fitzpatrick,[20] B. T. Fleming,[36] N. Foppiani,[13] D. Franco,[36] A. P. Furmanski,[21] D. Garcia-Gamez,[12] S. Gardiner,[11] G. Ge,[9] S. Gollapinni,[31,17] O. Goodwin,[18] E. Gramellini,[11] P. Green,[18] H. Greenlee,[11] W. Gu,[2] R. Guenette,[13] P. Guzowski,[18] L. Hagaman,[36] O. Hen,[19] C. Hilgenberg,[21] G. A. Horton-Smith,[15] A. Hourlier,[19] R. Itay,[26] C. James,[11] X. Ji,[2] L. Jiang,[34] J. H. Jo,[36] R. A. Johnson,[7] Y.-J. Jwa,[9] D. Kalra,[9] N. Kamp,[19] N. Kaneshige,[3] G. Karagiorgi,[9] W. Ketchum,[11] M. Kirby,[11] T. Kobilarcik,[11] I. Kreslo,[1] I. Lepetic,[25] K. Li,[36] Y. Li,[2] K. Lin,[17] B. R. Littlejohn,[14] W. C. Louis,[17] X. Luo,[3] K. Manivannan,[29] C. Mariani,[34] D. Marsden,[18] J. Marshall,[35] D. A. Martinez Caicedo,[27] K. Mason,[33] A. Mastbaum,[25] N. McConkey,[18] V. Meddage,[15] T. Mettler,[1] K. Miller,[6] J. Mills,[33] K. Mistry,[18] A. Mogan,[31] T. Mohayai,[11] J. Moon,[19] M. Mooney,[8] A. F. Moor,[4] C. D. Moore,[11] L. Mora Lepin,[18] J. Mousseau,[20] M. Murphy,[34] D. Naples,[24] A. Navrer-Agasson,[18] M. Nebot-Guinot,[10] R. K. Neely,[15] D. A. Newmark,[17] J. Nowak,[16] M. Nunes,[29] O. Palamara,[11] V. Paolone,[24] A. Papadopoulou,[19] V. Papavassiliou,[22] S. F. Pate,[22] N. Patel,[16] A. Paudel,[15] Z. Pavlovic,[11] E. Piasetzky,[30] I. D. Ponce-Pinto,[36] S. Prince,[13] X. Qian,[2] J. L. Raaf,[11] V. Radeka,[2] A. Rafique,[15] M. Reggiani-Guzzo,[18] L. Ren,[22] L. C. J. Rice,[24] L. Rochester,[26] J. Rodriguez Rondon,[27] M. Rosenberg,[24] M. Ross-Lonergan,[9] G. Scanavini,[36] D. W. Schmitz,[6] A. Schukraft,[11] W. Seligman,[9] M. H. Shaevitz,[9] R. Sharankova,[33] J. Shi,[4] J. Sinclair,[1] A. Smith,[4] E. L. Snider,[11] M. Soderberg,[29] S. Söldner-Rembold,[18] P. Spentzouris,[11] J. Spitz,[20] M. Stancari,[11] J. St. John,[11] T. Strauss,[11] K. Sutton,[9] S. Sword-Fehlberg,[22] A. M. Szelc,[10] W. Tang,[31] K. Terao,[26] C. Thorpe,[16] D. Totani,[3] M. Toups,[11] Y.-T. Tsai,[26] M. A. Uchida,[4] T. Usher,[26] W. Van De Pontseele,[23,13] B. Viren,[2] M. Weber,[1] H. Wei,[2] Z. Williams,[32] S. Wolbers,[11] T. Wongjirad,[33] M. Wospakrik,[11] K. Wresilo,[4] N. Wright,[19] W. Wu,[11] E. Yandel,[3] T. Yang,[11] G. Yarbrough,[31] L. E. Yates,[19] H. W. Yu,[2] G. P. Zeller,[11] J. Zennamo,[11] and C. Zhang[2]

(MicroBooNE Collaboration)[*]

[1]*Universität Bern, Bern CH-3012, Switzerland*
[2]*Brookhaven National Laboratory (BNL), Upton, New York 11973, USA*
[3]*University of California, Santa Barbara, California 93106, USA*
[4]*University of Cambridge, Cambridge CB3 0HE, United Kingdom*
[5]*Centro de Investigaciones Energéticas, Medioambientales y Tecnológicas (CIEMAT), Madrid E-28040, Spain*
[6]*University of Chicago, Chicago, Illinois 60637, USA*
[7]*University of Cincinnati, Cincinnati, Ohio 45221, USA*
[8]*Colorado State University, Fort Collins, Colorado 80523, USA*
[9]*Columbia University, New York, New York 10027, USA*
[10]*University of Edinburgh, Edinburgh EH9 3FD, United Kingdom*
[11]*Fermi National Accelerator Laboratory (FNAL), Batavia, Illinois 60510, USA*
[12]*Universidad de Granada, Granada E-18071, Spain*
[13]*Harvard University, Cambridge, Massachusetts 02138, USA*
[14]*Illinois Institute of Technology (IIT), Chicago, Illinois 60616, USA*
[15]*Kansas State University (KSU), Manhattan, Kansas 66506, USA*
[16]*Lancaster University, Lancaster LA1 4YW, United Kingdom*
[17]*Los Alamos National Laboratory (LANL), Los Alamos, New Mexico 87545, USA*
[18]*The University of Manchester, Manchester M13 9PL, United Kingdom*
[19]*Massachusetts Institute of Technology (MIT), Cambridge, Massachusetts, 02139, USA*
[20]*University of Michigan, Ann Arbor, Michigan 48109, USA*
[21]*University of Minnesota, Minneapolis, Minnesota 55455, USA*
[22]*New Mexico State University (NMSU), Las Cruces, New Mexico 88003, USA*
[23]*University of Oxford, Oxford OX1 3RH, United Kingdom*
[24]*University of Pittsburgh, Pittsburgh, Pennsylvania 15260, USA*
[25]*Rutgers University, Piscataway, New Jersey 08854, USA*

[26]*SLAC National Accelerator Laboratory, Menlo Park, California 94025, USA*
[27]*South Dakota School of Mines and Technology (SDSMT), Rapid City, South Dakota 57701, USA*
[28]*University of Southern Maine, Portland, Maine 04104, USA*
[29]*Syracuse University, Syracuse, New York 13244, USA*
[30]*Tel Aviv University, Tel Aviv 69978, Israel*
[31]*University of Tennessee, Knoxville, Tennessee 37996, USA*
[32]*University of Texas, Arlington, Texas 76019, USA*
[33]*Tufts University, Medford, Massachusetts 02155, USA*
[34]*Center for Neutrino Physics, Virginia Tech, Blacksburg, Virginia 24061, USA*
[35]*University of Warwick, Coventry CV4 7AL, United Kingdom*
[36]*Wright Laboratory, Department of Physics, Yale University, New Haven, Connecticut 06520, USA*

(Received 1 November 2021; accepted 16 February 2022; published 4 April 2022)

Obtaining a high-quality interaction model with associated uncertainties is essential for neutrino experiments studying oscillations, nuclear scattering processes, or both. As a primary input to the MicroBooNE experiment's next generation of neutrino cross section measurements and its flagship investigation of the MiniBooNE low-energy excess, we present a new tune of the charged-current pionless (CC0$\pi$) interaction cross section via the two major contributing processes—charged-current quasielastic and multinucleon interaction models—within version 3.0.6 of the GENIE neutrino event generator. Parameters in these models are tuned to muon neutrino CC0$\pi$ cross section data obtained by the T2K experiment, which provides an independent set of neutrino interactions with a neutrino flux in a similar energy range to MicroBooNE's neutrino beam. Although the fit is to muon neutrino data, the information carries over to electron neutrino simulation because the same underlying models are used in GENIE. A number of novel fit parameters were developed for this work, and the optimal parameters were chosen from existing and new sets. We choose to fit four parameters that have not previously been constrained by theory or data. Thus, this will be called a theory-driven tune. The result is an improved match to the T2K CC0$\pi$ data with more well-motivated uncertainties based on the fit.

DOI: 10.1103/PhysRevD.105.072001

## I. INTRODUCTION

A fundamental challenge in a large variety of accelerator experiments is to have an accurate Monte Carlo (MC) simulation of the apparatus. For neutrino experiments, a key aspect is the neutrino interaction modeling [1]. For MicroBooNE [2], this is true both for the low-energy excess (LEE) search [3–7] (based on the findings of MiniBoone [8]) and neutrino-argon scattering cross section measurements. MicroBooNE uses a liquid argon target exposed to Fermilab's booster neutrino beam, which has a mean neutrino energy of 0.8 GeV [9]. This makes the LEE search sensitive to nuclear effects such as multinucleon correlations and medium corrections. Cross section measurements require a model that can provide a reliable estimate of the contribution of background events in a selection. Although selection cuts that decrease the number of background events and data-driven estimations are highly desirable, problems with background very often remain and the model-data correspondence must be close enough to trust the efficiency estimation. MicroBooNE's LEE search, on the other hand, has the critical requirement of a model that provides a baseline estimate for most non-LEE contributions to the event yields and estimated uncertainties. The model also correlates uncertainties between different samples of selected events. Achieving significant improvement in the understanding of both the central-value model and its related uncertainties is the most important goal of this work.

The MicroBooNE dataset contains a significant number of charged-current quasielastic (CCQE) interactions, as well as charged-current two-particle, two-hole (CC2p2h) interactions in which the neutrino interacts with a correlated pair of nucleons. Resonant (RES) interactions, particularly resonant pion production, also form a considerable portion of the interactions collected by MicroBooNE (although these interactions tend to be at the highest energies in the neutrino flux and therefore of less concern for MicroBooNE's electronlike LEE searches) and deep inelastic scattering (DIS) also occurs in smaller proportions at even higher energies. MicroBooNE has adopted GENIE [10] v3.0.6 G18_10$a$_02_11$a$ as its core event generator at this time. This version of GENIE uses new models from the Valencia group [11–13] for CCQE and CC2p2h processes. The introduction of new models presents the problem of

*microboone_info@fnal.gov

choosing features of the model to test. We develop a theory-driven set of parameters for this purpose where the parameters are chosen with respect to the lack of understanding in the underlying theory.

The treatment of nuclear dependence (or $A$ dependence) is important to this work because the existing data are largely for carbon targets and the MicroBooNE detector is almost totally composed of argon. Because GENIE is required to simulate interactions with the wide variety of nuclei used in experiments, it needs a simple nuclear model. Neutrinos interact weakly within nuclei and linear dependence on A is then used. In GENIE, corrections come in two ways. All hadrons are subject to final state interactions which have a basic $\sim A^{2/3}$ dependence on nucleus. Corrections for the binding energy of the struck nucleon [14] and medium dependence in FSI [15] are applied; both have weak A dependence. All medium corrections have a smooth dependence on A and are determined in fits to inclusive and semi-inclusive electron scattering data.

In this article, we present a tune of the GENIE [10] v3.0.6 G1810$a$0211$a$ CCQE and CC2p2h models to T2K CC0$\pi$ cross section data [16]. The main purpose of this work is to provide an important input to the $\nu_e$-focused MicroBooNE LEE analyses [3–6]. One of the primary goals there is to use the $\nu_\mu$ data to constrain the $\nu_e$ model with robust uncertainties and covariances. The goal is to propagate features properly across channels and this fit is the basis for that exercise.

Although we tune underlying model parameters of these specific processes, the aim of this work is to improve the prediction of the overall CC0$\pi$ cross section, and thereby improve the model predictions and uncertainties used in MicroBooNE analyses. The signal choice of CC0$\pi$ means no mesons in the final state; experiments use this choice because it has less model dependence than true CCQE (which cannot be directly measured in a neutrino experiment). It includes CCQE, CC2p2h, and some pion production (where the pion is absorbed in the residual nucleus) events.

The choice of the dataset to study here is an important decision that is particular to the MicroBooNE experiment. Tuning to external data (i.e., data from another experiment) allows us to avoid any potential biases from double-fitting to MicroBooNE data in any subsequent analyses. Although choices of target and beam energy must be considered, the emphasis is on external datasets with similar beam energy because the number and complexity of allowed interaction channels grow as the beam energy increases. The T2K [16–20] and MiniBooNE [21,22] experiments both have CC0$\pi$ data sets with neutrino fluxes in a very similar energy range to MicroBooNE (in fact, the MiniBooNE experiment sits in the same beam line as MicroBooNE and sees an almost identical neutrino flux). MINERvA has also published CC0$\pi$ data [23–29], but this selection has a high proportion of RES and DIS interactions due to the larger neutrino energies. It should also be noted that all three experiments use a CH (scintillator plastic) target (T2K also has some water-target data), whereas MicroBooNE uses an argon target. ArgoNeuT data [30,31] uses an argon target, but is at a higher energy and has significant statistical uncertainties.

Restricting the study to neutrino energies below 2 GeV limits consideration to the CCQE and CC2p2h models. This would imply looking at data from the T2K and MiniBooNE experiments. However, there is one more consideration: independence of the data used for tuning from other MicroBooNE simulations and analyses. MiniBooNE is also located in the booster neutrino beam line at Fermilab, in a similar location to MicroBooNE. Both experiments see an almost-identical neutrino flux and use the same simulation to calculate the neutrino flux prediction and uncertainties. This means that the flux uncertainties included in the reported MiniBooNE cross section data will be extremely correlated with those used in MicroBooNE analyses. This issue of correlations between the two measurements is complicated: if not handled properly, it runs the risk of double counting uncertainties or propagating unknown biases from incorrect or misunderstood calculations. Correctly accounting for shared simulation components between published MiniBooNE cross section data and ongoing MicroBooNE analyses is currently infeasible, so we restrict our focus in model tuning to data from T2K. Considering T2K data alone minimizes the risk that the data used for tuning would be correlated with subsequent MicroBooNE analysis inputs.

Nevertheless, MiniBooNE CC0$\pi$ data are still important for this work. These data have provided an important basis for understanding interaction mechanisms in this energy range, and have informed the model choices in GENIE. While we do not tune to data from either MiniBooNE or MicroBooNE, comparisons of the nominal and tuned GENIE predictions with these data are a powerful tool to evaluate the tuned models, and therefore are shown in Secs. II, IV B (MiniBooNE), and IV A (MicroBooNE).

This work was required because the default GENIE v3.0.6 G1810$a$0211$a$ model configuration was found to underpredict cross section data from various experiments for charged-current interactions that produce no charged or neutral pions above detection threshold (the CC0$\pi$ channel, which is dominated by CCQE and CC2p2h interactions). This is discussed further in Sec. II. The features of GENIE that are important for this fitting exercise are also presented in Sec. II.

The data chosen for tuning and selection of parameters needed to properly tune the model for MicroBooNE are described in Sec. III. Fit results are presented in Sec. IV along with comparisons to other relevant data. A full description of MicroBooNE's adopted set of neutrino cross section model uncertainties is given in Sec. V, and the conclusions from this study are summarized in Sec. VI.

## II. GENIE MODELS

The latest version of GENIE (v3) [32] has a variety of model sets available to allow users to make the best choice for their particular analysis. The GENIE v3.0.6 G1810$a$0211$a$ model set includes the full Valencia model [11–13] for the local Fermi gas nucleon momentum distribution, CCQE, and CC2p2h interactions. This adds the RPA correction (random phase approximation, which is a description of long-range nucleon-nucleon correlations) and the Coulomb interaction of the outgoing muon. It also includes improved agreement with a significantly expanded dataset for the $A$ dependence of final state interactions (FSI) along with updated form factors [33] and diagrams for the pion production process [34–36]. A new tune to neutrino-proton and neutrino-deuterium cross section data [37] has been applied. These features represent significant enhancements for neutrino energies sampled by MicroBooNE over the historical default model from GENIE v2.12.2 (used by previous MicroBooNE analyses [38–41]).

The Valencia models as implemented in GENIE v3 are somewhat different than those in the original publications [11–13] outlining the Valencia models. The CC2p2h model had a restriction on the 3-momentum transfer [13] which has little effect at lower neutrino energies. The CCQE model [12] applied a simple binding energy correction by subtracting it from the muon energy. GENIE v3 used a more detailed method of decreasing the effective mass of the struck nucleon [14,32]. This feature will have an important impact on the analysis presented here.

The updated models have been validated against both inclusive and exclusive bubble-chamber experiments, and provide a significantly improved description of CC0$\pi$ cross section data from MiniBooNE [22] compared to the GENIE v2.12.2 models. The relativistic Fermi gas nuclear model and Llewellyn-Smith QE model used in GENIE v2.12.2 are more appropriate for measurements at a higher beam energy than the booster neutrino beam energies. Figure 1 shows a comparison of MiniBooNE CC0$\pi$ data [22] with simulations from these two models. GENIE v3.0.6 G1810$a$0211$a$ more closely matches the data and will be the basis for the fit we describe in this document. However, it is also clear that GENIE v3.0.6 G1810$a$0211$a$ underpredicts the data in both angular bins shown $[-0.1 < \cos(\theta_\mu) < 0.0$ and $0.9 < \cos(\theta_\mu) < 1.0]$ where $\theta_\mu$ is the lab angle of the muon with respect to the best estimate of the neutrino direction. Table I provides a $\chi^2$ analysis of these two bins using the shape and normalization uncertainties provided by the collaboration. A similar underprediction can be seen when comparing to CC0$\pi$ cross section data from T2K [16] in Fig. 2, as well as in data selections for MicroBooNE, such as that shown in Fig. 9(a). The underproduction of MicroBooNE data is the primary motivation for this tuning work in the context of the LEE search.

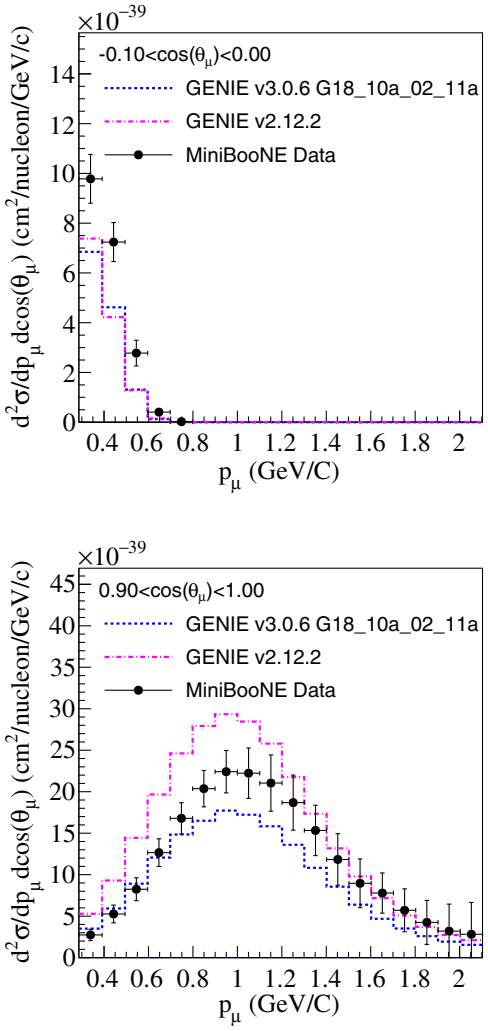


FIG. 1. MiniBooNE flux-averaged CC0$\pi$-like differential cross section [22] for muon kinetic energy $p_\mu$ compared with GENIE v2.12.2 and v3.0.6 G18_10$a$_02_11$a$ simulations for $-0.1 < \cos\theta_\mu < 0.0$ (top) and $0.9 < \cos\theta_\mu < 1.0$ (bottom). The original data release is in terms of muon kinetic energy. Uncertainties on the data points are the shape uncertainties reported by the collaboration. Uncertainties reported include a 10.7% normalization error and a $\chi^2$ analysis is presented in Table I. These bins show the underprediction of GENIE v3.0.6 G1810$a$0211$a$ compared to data for forwards-going and backwards-going muons.

The choice to tune specifically the CCQE and CC2p2h models in this work is motivated by several factors. The largest difference between data and simulation in many MicroBooNE analyses is seen at low visible energy [see, for example, Fig. 9(a)] where these interactions dominate. The lack of consensus about the optimal choice of these models in the theoretical community [1,42–44] strongly drives the parameter choices in this fitting exercise. Tuning other channels (e.g., resonant pion production) has lower priority for MicroBooNE at this time, mainly because the contribution of these channels is less relevant for

TABLE I. $\chi^2$ for comparisons of GENIE v2.12.2 and v3.0.6 G18_10a_02_11a to MiniBooNE flux-averaged CC0$\pi$-like differential cross section data [22] for the two bins presented in Fig. 1. Following the information presented in the publication, $\chi^2$ are calculated separately for shape and normalization components, including a reported 10.7% normalization error. Each value is then presented in the table. No correlations between bins were included.

| $\chi^2_{\text{shape}}/N_{\text{bins}}, \chi^2_{\text{norm}}/N_{\text{bins}}$ | GENIE v3.0.6 G18_10a_02_11a | GENIE v2.12.2 |
|---|---|---|
| $-0.10 < \cos(\theta_\mu) < 0.00$ | 35.11/4, 11.41 | 34.60/4, 10.97 |
| $0.90 < \cos(\theta_\mu) < 1.00$ | 24.03/18, 3.83 | 110.46/18, 6.59 |

MicroBooNE's electronlike LEE searches due to the energy range and the effective $\pi^0$ rejection achieved by these analyses. However, the work presented here may be extended to include tuning of other channels in the future.

## III. FITTING METHOD

Fits to T2K CC0$\pi$ cross section data [16] are performed to tune parameters within the GENIE v3.0.6 G18_10a_02_11a CCQE and CC2p2h models using the GENIE reweighting package v1.0.4. The main goal is to mitigate the underprediction observed in both MicroBooNE and MiniBooNE data. The tuning was performed using the NUISANCE software package [45].

### A. T2K dataset

The choice of the single data set to include in a fit is important as the data set must be as close as possible to the MicroBooNE data and contain a high proportion of CCQE and CC2p2h interactions. The inclusion of more data sets would have complicated the fit because of the incompatibilities that can be exposed [46]. It was also important to limit the fit to data at neutrino energies compatible

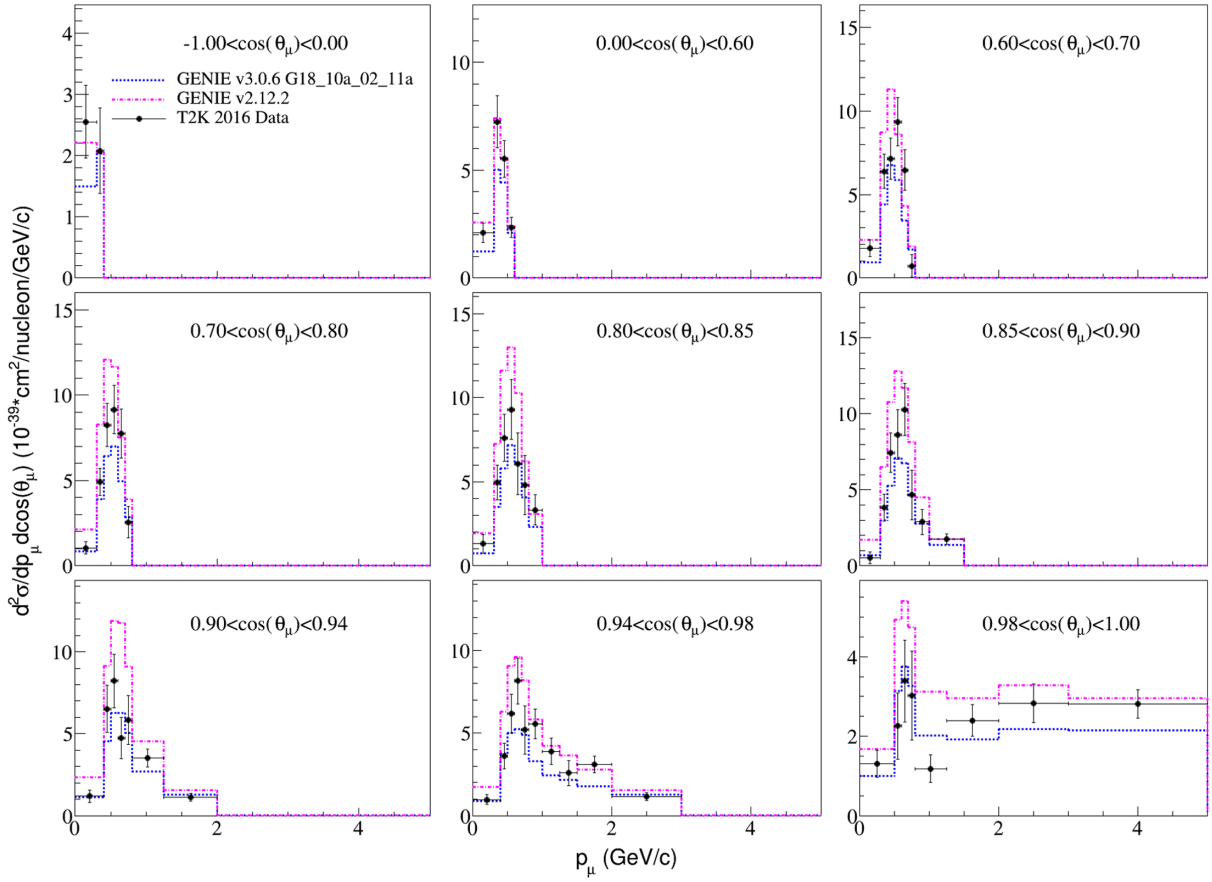


FIG. 2. T2K flux-averaged CC0$\pi$ analysis 1 double-differential cross section of lepton momentum and $\cos(\theta_\mu)$ [16] compared to nominal GENIE v3.0.6 G18_10*a*_02_11*a* ($\chi^2_{\text{diag}}/N_{\text{bins}} = 115.31/67$) and GENIE v2.12.2 ($\chi^2_{\text{diag}}/N_{\text{bins}} = 284.31/67$). The calculation of $\chi^2_{\text{diag}}$ uses only the uncertainties on the diagonals of the T2K CC0$\pi$ dataset. While only bins of $p_\mu < 5$ GeV are plotted, all bins with data up to $p_\mu = 30$ GeV are included in the $\chi^2_{\text{diag}}$ calculations.

with MicroBooNE because of the growing complexity of models needed to describe data properly as the energy increases [47].

We perform fits to T2K CC0$\pi$ cross section data, published in 2016 [16]. These results come from an analysis that requires an inclusive muon measurement. A later analysis of the same data includes results based on proton multiplicity [18]; for these fits the 2016 inclusive muon-based data are sufficient [16]. The paper includes two analyses, which both use the same data events but apply different selection cuts and extract the cross section using different methods:

(i) Analysis 1 uses a binned likelihood fit performed simultaneously in four signal and two control regions to extract the cross section. A 2D double-differential cross section as a function of muon momentum ($p_\mu$) and angle ($\cos\theta_\mu$) is provided in the full phase space.

(ii) Analysis 2 uses d'Agostini unfolding to extract the cross section. A 2D double-differential cross section as a function of muon momentum ($p_\mu$) and angle ($\cos\theta_\mu$) is provided in the restricted phase space where $p_\mu > 0.2$ GeV and $\cos\theta_\mu > 0.6$.

For the work presented in this article, we fit to "Analysis 1" from the paper, both because of the broader phase space of the "Analysis 1" result and because d'Agostini unfolding is known to produce undercoverage of uncertainties.

Figure 2 shows the complete T2K CC0$\pi$ analysis 1 data compared to GENIE v3.0.6 G18_10a_02_11a and GENIE v2.12.2. The data are presented in a double-differential cross section as a function of muon momentum ($p_\mu$) and angle ($\cos\theta_\mu$). We see the general pattern that the more recent GENIE prediction is below the T2K data, as we have also seen in MicroBooNE simulation.

The highest bin in muon momentum in each $\cos\theta$ bin is excluded in the fitting procedure because very high-momentum muons are not significant in the MicroBooNE analysis. In addition, the very small cross sections and small absolute uncertainties on the data in these bins can drive the fit in an undesirable way. This reduces the number of bins in the data fit from 67 (including high-muon momentum bins) to 58.

NUISANCE allows the use of the published bin-to-bin covariance matrix in the fitting process; this is generally regarded as the correct way to fit the data. Unfortunately, attempts to fit the T2K data with the full covariance matrix proved problematic, resulting in a significant and unphysical reduction of the cross section across all of the bins. Multiple hypotheses have been considered to explain this observation. We note that a recent publication in which NuWro models are fit to T2K and MINERvA data sees a similar effect when fitting the MINERvA data [44] and attributes it to Peelle's pertinent puzzle [48].

For the main result of this work, we avoided these problems with fits that use only diagonal elements of the full covariance matrix—corresponding to the error bars on each data point drawn in Fig. 2—and do not consider correlations between bins. As discussed in Sec. IV, additional tests using alternate methods [49] to include the effect of correlations were conducted to test the robustness of this approach.

### B. Parameter choice

When using the MINUIT fitting formalism, the choices of parameters to fit are limited because of the difficulty of finding a global minimum with reasonable uncertainties, especially when parameters are highly correlated. In addition, parameters should be chosen to reflect the underlying physics. This means choosing parameters that clearly show a particular physical effect that is not already constrained by data. For example, the CC2p2h contribution is uncertain and makes its study very useful to a variety of researchers.

The decision on parameters to avoid is also important. Although many other fitting exercises use the Fermi momentum as a free parameter [21], we ignored it because it is already well known from electron scattering and any significant differences between electron and neutrino probes are unlikely. Although the MicroBooNE LEE analysis is sensitive to protons in the final state, we do not use any FSI parameters for protons because the T2K 2016 data [16] contains only information on the muon. This is a limitation of this analysis; future work may find it beneficial to add FSI parameters in a fit to measurements of proton kinematics in the T2K data [18].

The reweighting package provided with GENIE allows tuning of the CCQE model via the parameter MaCCQE (which affects both shape and absolute normalization) and tuning of the CC2p2h model via an absolute normalization parameter. These are obvious choices to include in our tuning. We also consider a number of other parameters that we expect might have an effect on this dataset: some available in the GENIE reweighting package and some that were developed and added to GENIE for this work. Section III B 1 lists the parameters that were chosen to include in the fit to T2K data, and Sec. V A details additional new parameters that were developed for the MicroBooNE interaction uncertainty evaluation, but ultimately not included in the fits presented here.

#### *1. Fit parameters*

*MaCCQE.*—Axial mass in the dipole form factor used in the CCQE cross section calculation. Increasing this parameter's value has the effect of increasing the normalization of CCQE interactions, as well as changing the shape of the cross section as a function of $Q^2$, where Q is the 4-momentum transfer to the nucleus.

*CCQE RPA.*—GENIE v3.0.6 G18_10a_02_11a uses the Valencia RPA calculation to correct the CCQE cross section for nucleon-nucleon long range correlations.

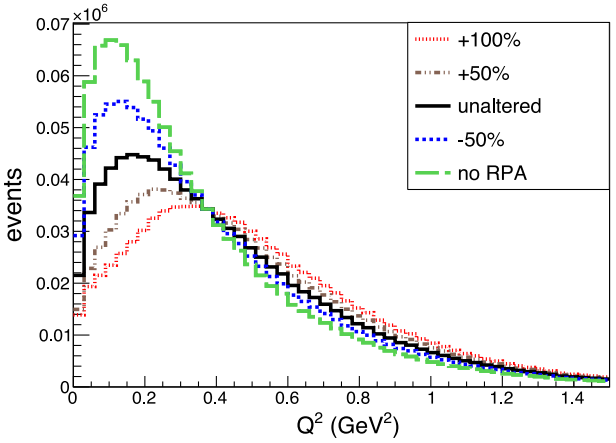


FIG. 3. GENIE v3.0.6 prediction of the true $Q^2$ distribution for $\nu_\mu$ CCQE scattering on $^{40}$Ar in MicroBooNE. The black histogram shows the untuned result for the G18_10*a*_02_11*a* model set, which includes Valencia RPA corrections to the CCQE cross section. The other histograms show alterations to the strength of the untuned CCQE RPA correction calculated via reweighting.

This manifests itself predominantly as a suppression of the CCQE cross section at low $Q^2$. There exists a large body of evidence in support of such a suppression, but calculations differ on its exact strength (including theoretical approximations used in the Valencia prediction), which is not currently well-constrained by data. A new GENIE reweighting parameter has been developed for this work that extrapolates linearly from the nominal RPA model (Valencia) to a model in which the RPA correction is turned off completely. Moving the parameter's value in the opposite direction strengthens the RPA suppression. Figure 3 illustrates the effect of applying the parameter to a sample of simulated $\nu_\mu$ CCQE events generated using a $^{40}$Ar target and the MicroBooNE flux. The low-$Q^2$ portion of the event distribution shows the expected suppression in the nominal model (black) relative to the "RPA correction off" model (green). The other histograms show further reweighting-based variations of the RPA strength which follow the expected trend.

Figure 4 and Table II show the impact of RPA corrections on predictions for CC0$\pi$ events at forward muon scattering angles (low $Q^2$) in T2K, changing between the untuned prediction (100% of the nominal RPA strength) and the "RPA correction off" prediction. The effect on the T2K distribution is significant and consistent with what we would expect; the overall effect of including RPA corrections is to improve the fit in one angle bin and make it worse in the other bin. Because of the large impact on the CCQE cross section and thus on the T2K prediction, we include this RPA parameter in the fits.

*CC2p2h normalization.*—This parameter changes the overall absolute normalization of the CC2p2h cross section. A parameter value of 1 corresponds to the default normalization of CC2p2h interactions in GENIE v3.0.6

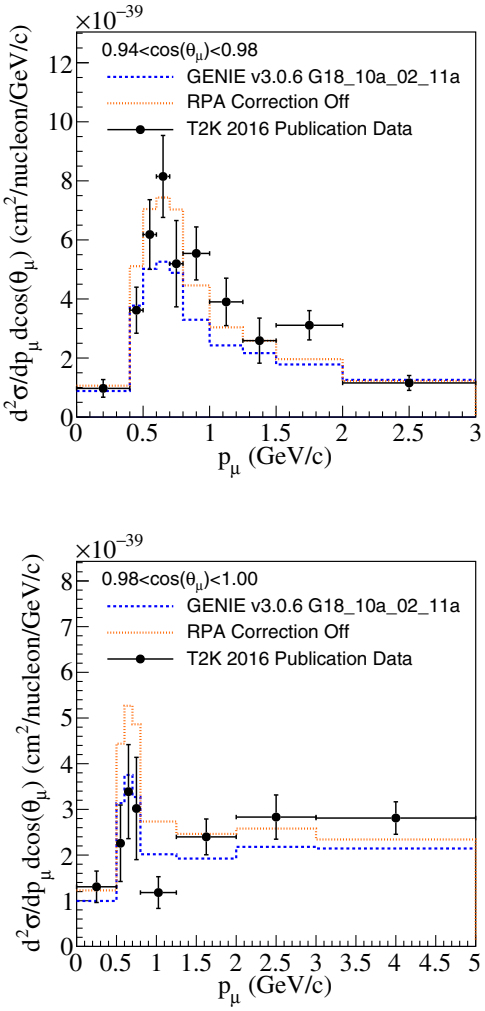


FIG. 4. T2K flux-averaged CC0$\pi$ analysis 1 data as a function of muon momentum for $0.94 < \cos(\theta_\mu) < 0.98$ (top) and $0.98 < \cos(\theta_\mu) < 1.00$ (bottom) compared to the nominal GENIE v3.0.6 G18_10*a*_02_11*a* prediction and the prediction with no CCQE RPA corrections. Both plots are enlarged on a lower range of muon momentum for readability, although all bins are included in the $\chi^2_{\text{diag}}$ calculations in Table II.

G18_10a_02_11a. A larger value increases the average cross section with no change in shape.

*CC2p2h shape.*—At present, there are substantial differences between alternative theoretical predictions of lepton kinematics on CC2p2h scattering. To account for this, a parameter developed for this work changes the

TABLE II. $\chi^2_{\text{diag}}$ for GENIE v3.0.6 G1810*a*0211*a* with and without the Valencia CCQE RPA corrections for T2K CC0$\pi$ data as shown in Fig. 4. Only the diagonal terms in the covariance matrix are used in the $\chi^2_{\text{diag}}$ calculation.

| $\chi^2_{\text{diag}}/N_{\text{bins}}$ | $0.94<\cos(\theta_\mu)<0.98$ | $0.98<\cos(\theta_\mu)<1.00$ |
|---|---|---|
| RPA correction | 23.0/11 | 16.2/9 |
| No RPA correction | 14.8/11 | 35.9/9 |

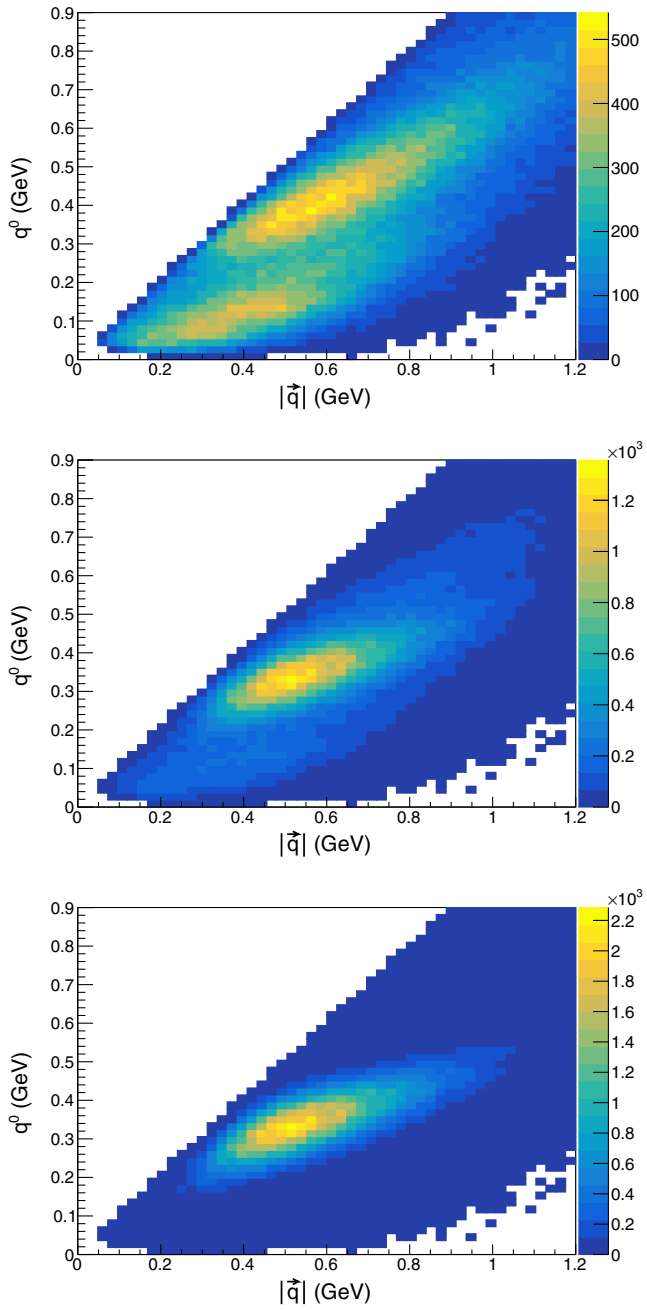


FIG. 5. Joint distribution (with arbitrary normalization) of the energy transfer ($q^0$) and magnitude of the three-momentum transfer ($|\vec{q}|$) for simulated $\nu_\mu$ CC2p2h events on $^{40}$Ar in MicroBooNE. Top: Valencia model prediction (CC2p2h shape dial at 0). Middle: intermediate prediction (CC2p2h Shape dial at 0.5). Bottom: GENIE empirical model prediction (CC2p2h shape dial at 1).

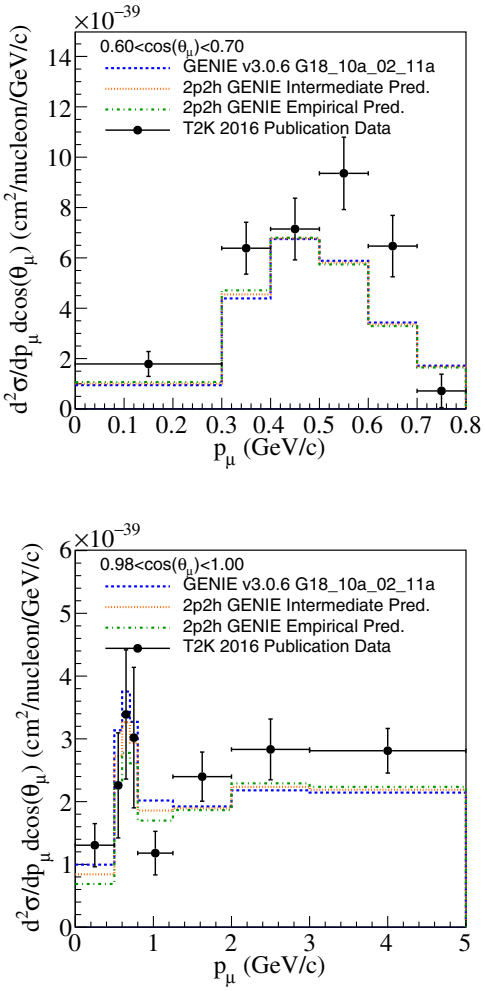


FIG. 6. T2K flux-averaged CC0$\pi$ analysis 1 cross section measurement as a function of muon momentum for $\cos(\theta_\mu)$ between $0.60 < \cos(\theta_\mu) < 0.70$ (top) and $0.98 < \cos(\theta_\mu) < 1.00$ (bottom) compared to the nominal GENIE v3.0.6 G18_10a_02_11a prediction with the Valencia model prediction (CC2p2h Shape dial at 0), the intermediate prediction (CC2p2h Shape dial at 0.5), and the GENIE empirical model prediction (CC2p2h shape dial at 1). Although neither plot shows the overflow bins for better understanding of the differences in performance, all bins are included in the $\chi^2_{\text{diag}}$ calculations in Table III.

shape of the inclusive CC2p2h differential cross section between the Valencia calculation [13] (the nominal model in our version of GENIE v3.0.6 G18_10a_02_11a, dial value = 0) and the GENIE Empirical model [50] (an alternative available in other GENIE configurations, dial value = 1). A linear interpolation is performed, which allows for continuous variations of the dial on the interval [0, 1]. The overall normalization of the cross section is left unaltered. Figure 5 illustrates the effect of the CC2p2h shape dial variations on the distribution of the leptonic energy and momentum transfer for simulated CC2p2h events in MicroBooNE. The two distinct peaks seen for the Valencia calculation (top plot) are replaced by a single peak (middle plot, dial value = 0.5) as the distribution is reshaped to resemble the GENIE Empirical model prediction (bottom plot) more closely. A similar kinematic distribution with a single peak is predicted by other CC2p2h models, e.g., SuSAv2-MEC [51].

Figure 6 shows the effect of changing the CC2p2h Shape dial from 0 (nominal) to 1 on the predicted CC0$\pi$ cross

TABLE III. $\chi^2_{\text{diag}}$ for GENIE v3.0.6 G1810$a$0211$a$ with the Valencia model prediction (CC2p2h shape dial at 0), the intermediate prediction (CC2p2h shape dial at 0.5), and the GENIE empirical model prediction (CC2p2h shape dial at 1) for flux-averaged T2K CC0$\pi$ analysis 1 data as shown in Fig. 6. Only the diagonal terms from the dataset covariance matrix are used for the $\chi^2_{\text{diag}}$ calculation.

| $\chi^2_{\text{diag}}/\text{N}_{\text{bins}}$ | $0.60 < \cos(\theta_\mu) < 0.70$ | $0.98 < \cos(\theta_\mu) < 1.00$ |
|---|---|---|
| Valencia CC2p2h | 21.9/7 | 16.2/9 |
| Intermediate CC2p2h | 21.2/7 | 13.5/9 |
| Empirical CC2p2h | 20.6/7 | 12.8/9 |

section at T2K. Although the CC2p2h shape change is subtle in some regions of phase space (top plot), it is an important effect in others (bottom plot). The sensitivity to shape of the muon angle-energy distribution is further corroborated in the $\chi^2_{\text{diag}}$ values reported in Table III. The CC2p2h shape parameter has a significant impact for MicroBooNE. Since the CC2p2h cross section shape is very much unknown, we include this parameter in our tuning.

The final parametrization for this tuning work consists of four parameters to be fit: MaCCQE, CC2p2h normalization, CCQE RPA strength, and CC2p2h shape.

## IV. FIT RESULTS

We fit four parameters (MaCCQE, CC2p2h normalization, CCQE RPA strength, and CC2p2h shape) to the T2K CC0$\pi$ cross section data, neglecting off-diagonal terms in the T2K data covariance matrix and the highest muon momentum bins (as described in Sec. III A). Table IV shows the results of three fits, adding in a parameter each time, such that the final row on the table shows the result of the full four-parameter fit (referred to in this article as the "MicroBooNE tune"). The fitted parameter values in this line are one of the primary results of this analysis. Postfit correlations between the parameters are shown in Fig. 7, and the tuned model is compared to the T2K data in Fig. 8. Agreement between data and simulation is measured as a $\chi^2_{\text{diag}}$ value across the whole dataset. As a result of the fit, the total $\chi^2_{\text{diag}}/\text{N}_{\text{bins}}$ is reduced from 115.3/67 to 63.8/67 (almost a factor of two) for the dataset using the errors from the diagonal of the covariance matrix. Using the full covariance matrix, the $\chi^2_{\text{full}}/\text{N}_{\text{bins}}$ is 155.2/67 for the "MicroBooNE tune" and 144.4/67 for the GENIE v3.0.6 G18_10a_02_11a prediction.

The fit results show increases in both MaCCQE (which in large part increases the CCQE cross section) and the CC2p2h cross section normalization. It favors a slight decrease in CCQE RPA strength (85% of nominal), albeit with a value consistent within a $1\sigma$ uncertainty of the Valencia prediction (100%). Interestingly, the fit prefers a CC2p2h shape in lepton kinematics that matches the empirical CC2p2h model over the Valencia prediction, although the fit uncertainty is close to the entire range of the parameter, indicating that the preference is not strong.

In Fig. 7, we find fairly strong anticorrelations between MaCCQE and CC2p2h normalization, because increasing MaCCQE increases the CCQE cross section normalization (with some additional changes in shape). Strong anticorrelations are also seen between the CC2p2h normalization and RPA strength parameters, which is to be expected because both have importance at forward muon angles. These anticorrelations suggest ambiguities in the tuning procedure, where different fitted parameters can have similar effects on the prediction. Therefore, one cannot assume that the central-value result of this tune has the correct ratio of contributions from the CCQE and CC2p2h processes. However, this tune does successfully adjust the overall rate and shape of the prediction in lepton kinematics for CC0$\pi$ interactions. Ambiguities between individual interaction processes can be correctly accounted for if the correlation matrix is taken into account in the treatment of uncertainties. The correlations between the CC2p2h normalization and shape parameters are small, consistent with the design of these parameters to be orthogonal.

TABLE IV. Tuned parameter values and uncertainties after fitting to T2K CC0$\pi$ data for the nominal simulation and three tunes that build to the final four parameter tune. Note that postfit $\chi^2$ values are quoted here only for the 58 bins included in the fit (excluding the highest muon momentum bin in each cos $\theta$ bin), and using diagonal elements of the covariance matrix only. In the text and figures, pre- and postfit $\chi^2$ comparisons are also quoted for the full T2K dataset of 67 bins. "Norm." is an abbreviation for normalization.

| | MaCCQE fitted value | CC2p2h Norm. fitted value | CCQE RPA Strength fitted value | CC2p2h Shape fitted value | T2K $\chi^2_{\text{diag}}/\text{N}_{\text{bins}}$ |
|---|---|---|---|---|---|
| Nominal (untuned) | 0.961242 GeV | 1 | 100% | 0 | 106.7/58 |
| Fit MaCCQE + CC2p2h Norm. | $1.14 \pm 0.07$ GeV | $1.61 \pm 0.19$ | 100% (fixed) | 0 (fixed) | 71.8/58 |
| Fit MaCCQE + CC2p2h Norm + CCQE RPA Strength | $1.18 \pm 0.08$ GeV | $1.12 \pm 0.38$ | $(64 \pm 23)\%$ | 0 (fixed) | 69.7/58 |
| Fit MaCCQE + CC2p2h Norm + CCQE RPA Strength + CC2p2h Shape | $1.10 \pm 0.07$ GeV | $1.66 \pm 0.19$ | $(85 \pm 20)\%$ | $1^{+0}_{-0.74}$ | 52.5/58 |

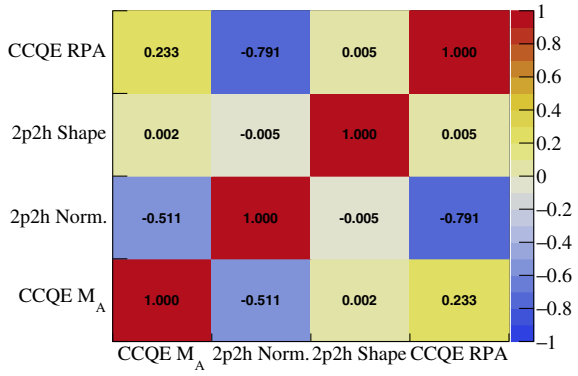


FIG. 7. Correlations between parameters after fitting to T2K CC0$\pi$ data.

Tests of the robustness of the fit are important. The variation of parameters in Table IV gives some indication of how choices of parameters impact the fit results. The variation of fit results as the number of parameters increases is not significant. The best-fit values for MaCCQE and CC2p2h normalization are fairly constant within uncertainties, with and without the shape parameters. The fitted value of CC2p2h normalization changes depending on the fitted value of RPA strength, which is consistent with the large anticorrelations between these parameters seen in the four-parameter fit covariance matrix.

As another test of robustness, the recent method of Koch [49] was used to include the effects of correlations between data bins. This method empirically separates the correlations into normalization (mostly due to uncertainties in neutrino flux calculations for neutrino experiments) and shape components when calculating the chi-squared ($\chi^2_{\text{Koch}}$). As a result, Peelle's pertinent puzzle can be mitigated. The best-fit parameter values obtained using this method are within the uncertainties provided by MINUIT of the values reported in Table V, with a difference of less than 10% in both $\chi^2_{\text{Koch}}$ and $\chi^2_{\text{diag}}$ with respect to the T2K data. Figure 8 shows only small differences bin-to-bin visually between the MicroBooNE tune and this "alternative fit." This gives evidence that the fitting method was reasonable.

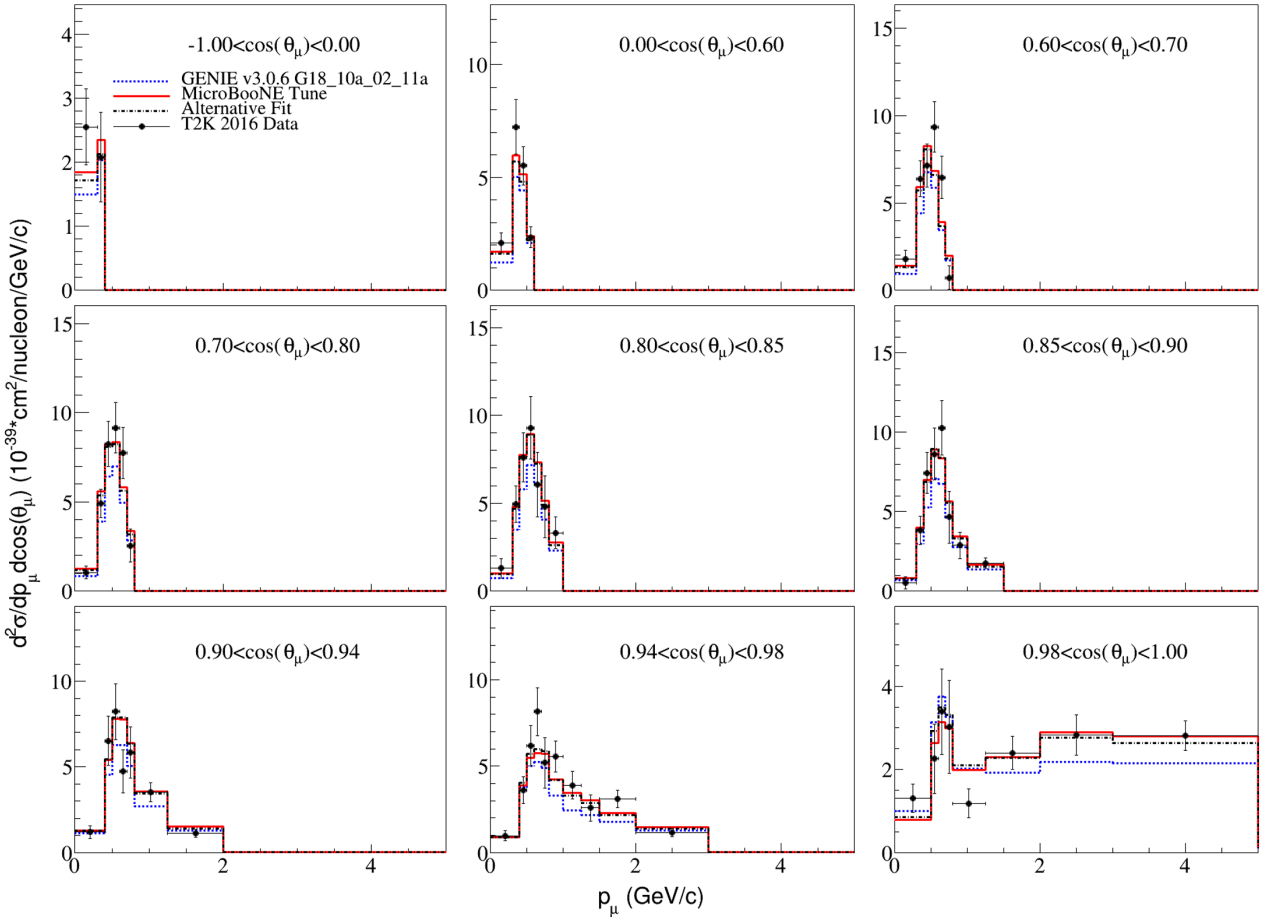


FIG. 8. T2K flux-averaged CC0$\pi$ double-differential cross section of lepton momentum and $\cos(\theta_\mu)$ [16] compared to GENIE v3.0.6 G18_10$a$_02_11$a$ ($\chi^2_{\text{diag}}/\text{N}_{\text{bins}} = 115.31/67$ bins), the "MicroBooNE tune" ($\chi^2_{\text{diag}}/\text{N}_{\text{bins}} = 63.77/67$ bins), and the "alternative fit" presented in Table V ($\chi^2_{\text{diag}}/\text{N}_{\text{bins}} = 63.52/67$ bins). Only the diagonal entries in the covariance matrix are used for the $\chi^2_{\text{diag}}$ evaluation. While only bins of $\text{p}_\mu < 5$ GeV are plotted, all bins with data up to $\text{p}_\mu = 30$ GeV are included in the $\chi^2_{\text{diag}}$ calculations.

TABLE V. Parameter values and uncertainties from nominal GENIE v3.0.6, the "MicroBooNE tune," and the "alternate fit." Postfit $\chi^2$ values are quoted only for the 58 bins included in the fit (excluding the highest muon momentum bin in each cos $\theta$ bin) using the diagonal elements of the covariance matrix only ($\chi^2_{\text{diag}}$), the Koch norm-shape covariance matrix [49] ($\chi^2_{\text{Koch}}$), and the full covariance matrix ($\chi^2_{\text{full}}$). Note that $\chi^2_{\text{diag}}$ is the figure-of-merit that is minimized in the "MicroBooNE tune" fit. "Norm." is an abbreviation for normalization.

| | MaCCQE fitted value | CC2p2h Norm. fitted value | CCQE RPA Strength fitted value | CC2p2h Shape fitted value | T2K $\chi^2_{\text{diag}}/N_{\text{bins}}$ | T2K $\chi^2_{\text{Koch}}/N_{\text{bins}}$ | T2K $\chi^2_{\text{full}}/N_{\text{bins}}$ |
|---|---|---|---|---|---|---|---|
| Nominal (untuned) | 0.961242 GeV | 1 | 100% | 0 | 106.7/58 | 149.83/58 | 97.56/58 |
| "MicroBooNE tune" | $1.10 \pm 0.07$ GeV | $1.66 \pm 0.19$ | $(85 \pm 20)$% | $1^{+0}_{-0.74}$ | 52.5/58 | 110.58/58 | 103.84/58 |
| "Alternate fit" | $1.04 \pm 0.10$ GeV | $1.44 \pm 0.42$ | $(67 \pm 16)$% | $0.91^{+0.09}_{-0.18}$ | 55.51/58 | 100.59/58 | 91.68/58 |

In addition, different parameters were chosen (e.g., CCQE normalization vs MaCCQE and different formulations of the shape parameters) with minimal change in the resulting agreement between data and simulation. In addition, alternate fits with different starting values, both small and random, give almost identical fit values and uncertainties. This gives confidence that the choice of fit parameters was robust.

The uncertainties shown in Table IV are the postfit uncertainties given by MINUIT. MicroBooNE analyses adopt uncertainties that cover the results of all three fits presented in Table IV: an uncertainty of 0.1 GeV on the parameter MaCCQE, 0.5 on the CC2p2h normalization, and 40% on the CCQE RPA strength. Because we expect MicroBooNE data to have a better ability to distinguish between 2p2h models than the T2K data, we adopt an uncertainty that covers the full allowed range of the parameter for CC2p2h shape: $1^{+0}_{-1}$.

### A. "MicroBooNE tune" comparison to MicroBooNE data

Because the aim of this tuning work is to support MicroBooNE analyses, it is important to compare the "MicroBooNE tune" to MicroBooNE data. While the T2K data are in a similar energy range to MicroBooNE, they are on a different nuclear target. Therefore it is imperative to check that the fitted result within uncertainties can predict MicroBooNE's measured argon-target interactions. Comparisons of the tuned and untuned GENIE v3 models to MicroBooNE data are provided in this section for generic neutrino scattering, $\nu_\mu$ CC inclusive events, and exclusive one-muon, one-proton ($1\mu 1p$) final states consistent with CCQE kinematics. The goal is to have meaningful comparisons, but no attempt is made to be comprehensive. As is the case for any neutrino interaction model, the suitability of the "MicroBooNE tune" (and its associated uncertainties) for any specific analysis must be determined on a case-by-case basis. Further data-driven model constraints will often be essential for achieving sufficient precision. However, based on the overall improvement seen in the description of MicroBooNE data across many event selections and observables, the collaboration has adopted the "MicroBooNE tune" described herein as the base neutrino interaction model for all current analyses, including those investigating the MiniBooNE LEE [3–7] and neutrino-argon cross sections [52,53].

Figure 9 shows the events selected in the MicroBooNE detector using the generic neutrino detection described

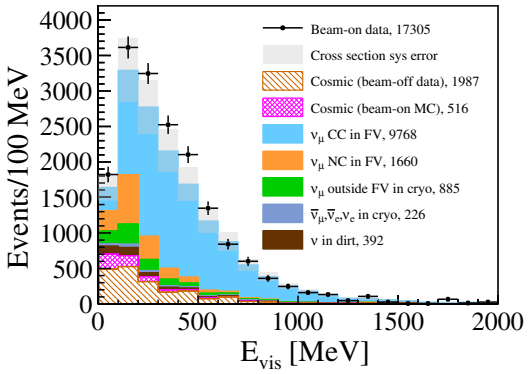


(a) Simulated neutrino interactions predicted by GENIE v3.0.6 G18_10a_02_11a

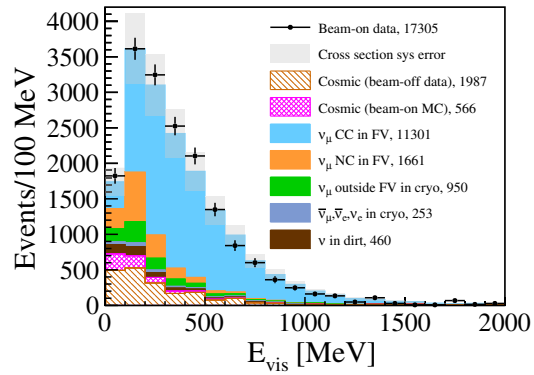


(b) Simulated neutrino interactions predicted by the "MicroBooNE Tune" applied to GENIE v3.0.6 G18_10a_02_11a

FIG. 9. Total visible energy of events selected in the MicroBooNE detector using the generic neutrino detection described in [54], compared to MicroBooNE simulation before and after the "MicroBooNE tune" has been applied. The gray area indicates uncertainties on the cross section model only (including uncertainties on the tuned parameters, the new uncertainties presented in Sec. V A, and other uncertainties as recommended by the GENIE collaboration). The tuned model shows significantly better agreement with the data.

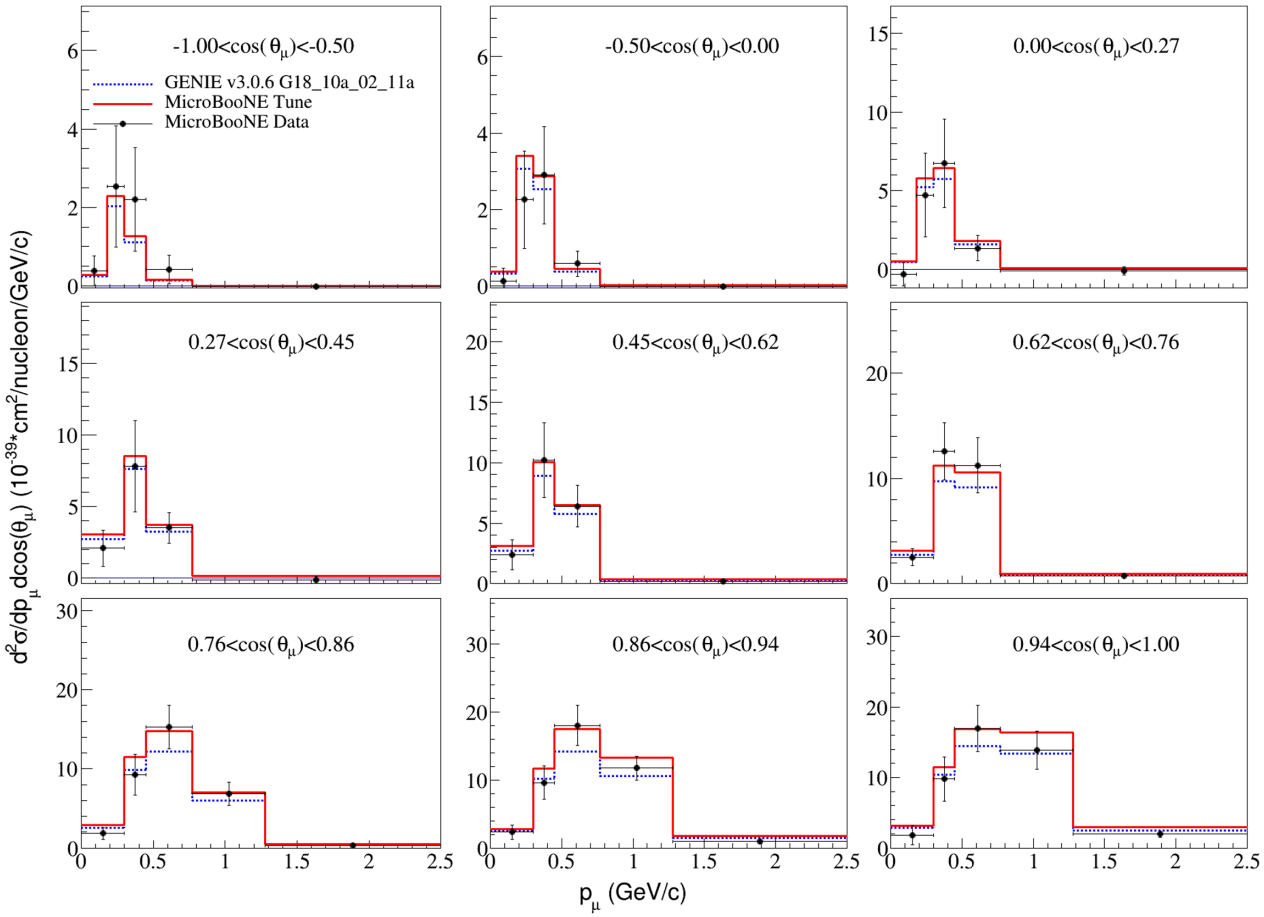


FIG. 10. MicroBooNE flux-averaged $\nu_\mu$ CC inclusive double-differential cross section as a function of muon momentum and $\cos(\theta_\mu)$ [55], compared to GENIE v3.0.6 G18_10a_02_11a ($\chi^2_{\text{full}}/\text{N}_{\text{bins}} = 105.41/42$) and the "MicroBooNE tune" central value ($\chi^2_{\text{full}}/\text{N}_{\text{bins}} = 140.55/42$) to T2K CC0$\pi$ data.

in Ref. [54], plotted as a function of visible energy. The same selected data events are shown in both panels, but the simulation uses untuned GENIE v3.0.6 G1810$a$0211$a$ in Fig. 9(a) and the simulation computed with the "MicroBooNE tune" is applied in Fig. 9(b). The tune increases the normalization of the simulation, decreasing the data/simulation ratio from 1.12 (untuned) to 1.01 ("MicroBooNE tune").

Figure 10 shows GENIE v3.0.6 G18_10a_02_11a and the "MicroBooNE tune" central value (neglecting uncertainties on the predictions) compared to the double-differential cross section for CC inclusive interactions measured in the MicroBooNE detector as a function of lepton momentum and $\cos(\theta_\mu)$ [55]. Table VI provides a comparison of $\chi^2_{\text{full}}$ values using the full covariance matrix for the complete dataset and binned in angle. As seen elsewhere, a major effect of the tune is to increase the normalization of the prediction. However, the value of $\chi^2_{\text{full}}/\text{N}_{\text{bins}}$ in Table VI for the full angular range increases from 105.41/42 (untuned GENIE prediction) to 140.55/42 ("MicroBooNE tune"). Although the match is poor in both

TABLE VI. $\chi^2$ for the results of this work in Fig. 10 relative to MicroBooNE CC inclusive double-differential data using the full covariance matrix of the dataset for $\chi^2_{\text{full}}$ calculations. Included are both $\chi^2_{\text{full}}$ values for the full dataset and for each slice of $\cos(\theta_\mu)$. The per-slice $\chi^2$ values reported here do not include correlations between different slices.

| $\chi^2_{\text{full}}/\text{N}_{\text{bins}}$ | GENIE v3.0.6 G18_10$a$_02_11$a$ | "MicroBooNE tune" |
|---|---|---|
| Full dataset | 105.41/42 | 140.55/42 |
| $-1.00 < \cos(\theta_\mu) < -0.50$ | 3.50/5 bins | 3.47/5 |
| $-0.50 < \cos(\theta_\mu) < 0.00$ | 2.80/5 bins | 3.07/5 |
| $0.00 < \cos(\theta_\mu) < 0.27$ | 4.54/5 bins | 4.15/5 |
| $0.27 < \cos(\theta_\mu) < 0.45$ | 2.95/4 bins | 2.61/4 |
| $0.45 < \cos(\theta_\mu) < 0.62$ | 2.37/4 bins | 2.09/4 |
| $0.62 < \cos(\theta_\mu) < 0.76$ | 7.73/4 bins | 8.36/4 |
| $0.76 < \cos(\theta_\mu) < 0.86$ | 10.89/5 bins | 7.92/5 |
| $0.86 < \cos(\theta_\mu) < 0.94$ | 34.36/5 bins | 43.90/5 |
| $0.94 < \cos(\theta_\mu) < 1.00$ | 7.60/5 bins | 12.41/5 |

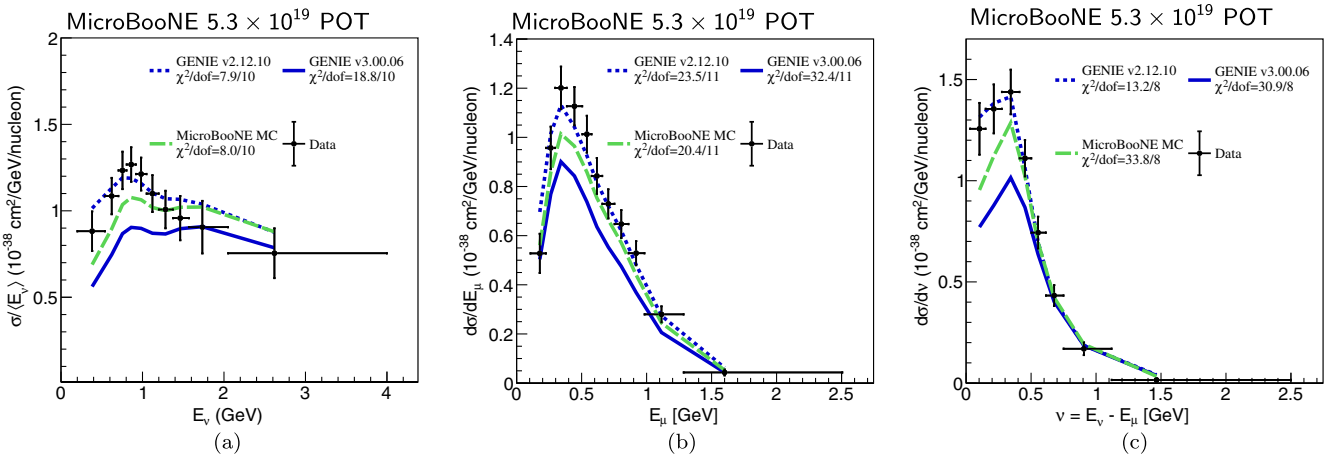


FIG. 11. Comparison of the GENIE v2.12.2 default model (dashed blue) and both the untuned (solid blue) and tuned (dashed green) GENIE v3.0.6 G18_10a_02_11a models to MicroBooNE measurements [53] of the $\nu_\mu$-argon CC inclusive cross section as a function of (a) neutrino energy, (b) muon energy, and (c) energy transfer. The data in plot (a) are divided by the bin-center neutrino energy. Chi-squared values are calculated while neglecting uncertainties on the model predictions.

cases, we find that the large $\chi^2_{\text{full}}/\text{N}_{\text{bins}}$ value is driven by the highest muon momentum bins for $\cos(\theta_\mu)$ approaching 1. For example, the measurement sits below both predictions and has a very small uncertainty in the highest muon momentum bin in the $0.86 \leq \cos(\theta_\mu) \leq 0.94$ angular bin. Removing this bin from the comparison gives an overall $\chi^2_{\text{full}}/\text{N}_{\text{bins}}$ of 69.7/41 (GENIE v3) or 90.2/41 ("MicroBooNE tune"). It also reduces the $\chi^2_{\text{full}}$ in the $0.86 \leq \cos(\theta_\mu) \leq 0.94$ angular bin to 6.2 (GENIE v3) or 8.3 ("MicroBooNE tune"). We find that the tuning has provided a better description of the data in some regions of phase space, notably at moderate muon production angles and momenta. However, there remains room for improvement in the description at high muon momentum and at very forward-going scattering angles. The alternative fit using [49] described in Sec. III results in a total $\chi^2_{\text{full}}/\text{N}_{\text{bins}}$ of 130.29/42, a 7.2% improvement over the "MicroBooNE tune" value. All the values of $\chi^2_{\text{full}}$ are large. As the $\chi^2_{\text{full}}/\text{N}_{\text{bins}}$ differ by less than one unit of $\chi^2_{\text{full}}$/bin across all three cases, we conclude that this shows approximately consistent agreement of all three model sets with these data.

Comparisons of the GENIE v2.12.10 default model, untuned GENIE v3.0.6 G18_10a_02_11a, and the "MicroBooNE tune" to additional MicroBooNE $\nu_\mu$ CC inclusive cross section measurements from Ref. [53] are shown in Fig. 11. These data were analyzed differently than the CC inclusive in Fig. 10 and plotted in different variables. When the theoretical uncertainties on each model prediction are neglected, the overall agreement between the data and the "MicroBooNE tune" is found in Figs. 10(a) and 10(b) to be comparable to or better than the two alternative GENIE models studied. For Fig. 10(c), the measurement of the differential cross section as a function of energy transfer ($d\sigma/d\nu$), the $\chi^2_{\text{full}}/\text{N}_{\text{bins}}$ value for the tune is slightly higher than untuned GENIE v3 and substantially higher than GENIE v2. Nevertheless, detailed studies of the tuned model, reported in Refs. [6,53], demonstrate that it provides a reliable description of MicroBooNE data in the low-$\nu$ region when theoretical uncertainties are taken into account.

As an example of the performance of the tuned model when confronted with a MicroBooNE measurement of a highly exclusive event topology, Fig. 12 compares the untuned (top panel) and tuned (bottom panel) GENIE model predictions to the reconstructed neutrino energy distribution obtained for the $1\mu 1p$ constraint sample used in the quasielastic $\nu_e$ LEE search [5]. The selection used here obtains a highly pure sample of $\nu_\mu$ CCQE events by checking the kinematic consistency of the $1\mu 1p$ final state with a two-body CCQE hypothesis. Application of the "MicroBooNE tune" substantially improves the level of GENIE model agreement with these data: a ratio of $1.23 \pm 0.13$ between the integrated data and the untuned model is reduced to $1.08 \pm 0.13$ with the tune, and the combined Neyman-Pearson chi-square ($\chi^2_{\text{CNP}}$) metric [56] for goodness-of-fit improves from $\chi^2_{\text{CNP}} = 32.00/19$ bins to $\chi^2_{\text{CNP}}/\text{N}_{\text{bins}} = 24.96/19$ [5]. Similar levels of improvement are seen for other kinematic distributions obtained using the same dataset. The agreement in this sample provides a valuable indication of the success of the "MicroBooNE tune" in describing CCQE interactions.

### B. "MicroBooNE tune" comparison to MiniBooNE data

We next compare the result of this tuning to data from the MiniBooNE experiment. Because this article presents a tune of the CCQE and CC2p2h parameters, we compare to measured CCQE-like cross section data [22], shown in

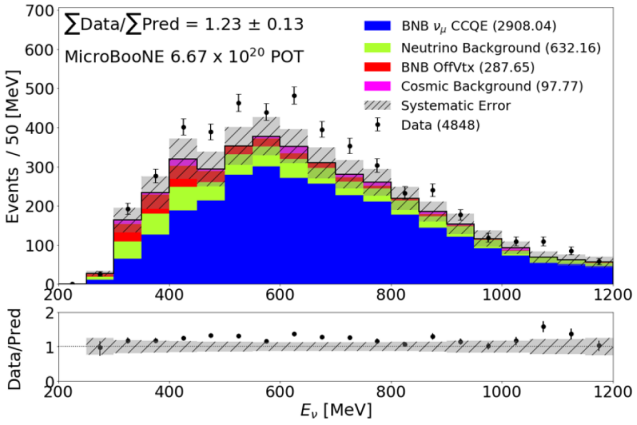


(a) Simulated neutrino interactions predicted by GENIE v3.0.6 G18_10a_02_11a ($\chi^2_{CNP}/\mathrm{N_{bins}} = 32.00/19$)

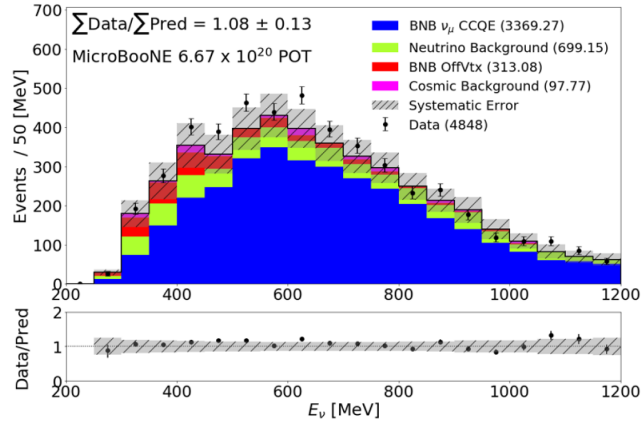


(b) Simulated neutrino interactions predicted by the "MicroBooNE Tune" applied to GENIE v3.0.6 G18_10a_02_11a ($\chi^2_{CNP/\mathrm{N_{bins}}=24.96/19}$)

FIG. 12. Reconstructed neutrino energy of $1\mu 1p$ events selected as input to a constraint for the MicroBooNE $1e1p$ LEE analysis described in Ref. [5]. The bottom panel is taken directly from that publication and uses the "MicroBooNE tune" of GENIE, while the top panel provides a similar comparison to the untuned GENIE v3.0.6 G18_10a_02_11a prediction. The gray hashed region in both indicates uncertainties on the model prediction (including uncertainties on the cross section modeling, detector modeling, and neutrino flux), and the quoted $\chi^2$ includes all uncertainties. Significantly better agreement with the data is achieved with the tuned GENIE model.

Fig. 13. The "CCQE-like" signal definition used by the MiniBooNE collaboration in [22] is consistent with what has been termed "CC0$\pi$" in this article: any interaction in which one muon, any number of nucleons, and no other particles are produced.

Figure 13 shows the comparison of tuned and untuned GENIE to the extracted CC0$\pi$ double-differential cross section measurement from MiniBooNE [22] as a function of lepton kinetic energy and $\cos(\theta_\mu)$. A $\chi^2$ analysis is given in Table VII. We see overall improved agreement when using the "MicroBooNE tune." More specifically, we see very good agreement for high energy muons, but the tuned model still underpredicts the data for low-energy muons. The original Valencia publications [11] had very good visual agreement with this data, although required a normalization shift of ∼10%. Using the GENIE version of the Valencia model [13] and the "MicroBooNE tune," no normalization shift is needed and, thus, the overall agreement is better. However, the ability to describe these low energy features is not as good as the original Valencia model [11] despite the use of an improved binding energy technique in GENIE. The application of a constant binding energy in GENIE [derived from $(e, e')$ data at higher energies [57] ] may still be a problem. A more realistic treatment would have binding energy depending on kinematics or the use of a spectral function, neither of which is included yet in GENIE.

It is interesting to note that we do not see a similar underprediction when comparing to the T2K data. In fact, attempts to tune to this MiniBooNE data have resulted in a prediction that is in tension with the T2K data, so we believe this represents an underlying tension between the two datasets.

## V. INTERACTION MODEL UNCERTAINTIES

The analysis presented in the preceding sections obtained refined values of four cross section model parameters describing the CC0$\pi$ channel, which is dominant in MicroBooNE. A complete treatment of neutrino interaction model uncertainties, however, requires a consideration of many additional degrees of freedom. This section documents the full set of neutrino cross section systematic uncertainties adopted in current MicroBooNE analyses. With the exception of CCQE uncertainties related to second-class currents (see Sec. V B), these are implemented by adding MicroBooNE-specific enhancements to the Reweight package [58] distributed with GENIE v3.0.6. These will be contributed by MicroBooNE for inclusion in the upcoming v3.2.0 release of GENIE.

The GENIE Reweight code provides a standard framework for evaluating model uncertainties via event reweighting: the impact of a model parameter variation on an existing sample of simulated events is approximated by assigning a numerical weight $w$ to each event equal to the likelihood ratio

$$w = L'/L. \tag{1}$$

Here $L$ is the likelihood of generating the event under the original GENIE configuration and $L'$ is the corresponding likelihood calculated after one or more interaction model parameters have been altered from their original values. Uncertainties on distributions calculated using the events may then be evaluated by comparing results obtained with different sets of event weights.

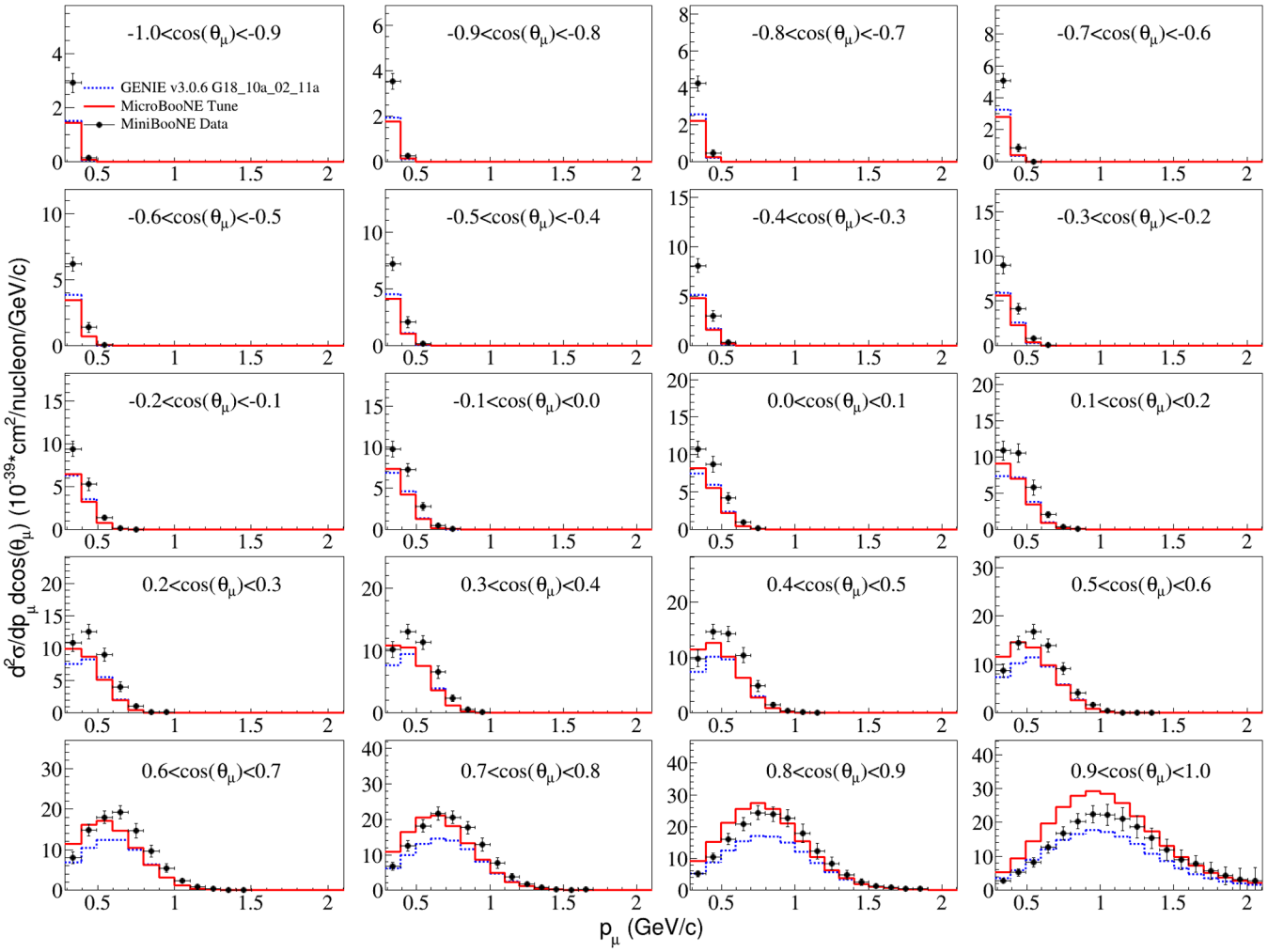


FIG. 13. MiniBooNE flux-averaged CCQE-like double-differential cross section as a function of muon momentum and $\cos(\theta_\mu)$ [22] compared to GENIE v3 and the"MicroBooNE tune." The original data release is in terms of muon kinetic energy. Uncertainties on the data points are the shape uncertainties reported by the collaboration. Table VII reports the $\chi^2$ values for both the shape and normalization between the predictions and the data reported in [22].

A typical uncertainty quantification method used by MicroBooNE is the multiple universe approach: a covariance matrix $V_{ij}$ describing the uncertainty on a vector of predicted event counts $n_i$ is constructed via the formula

$$V_{ij} = \frac{1}{N}\sum_{k=1}^{N}(n_i^k - n_i^{CV})(n_j^k - n_j^{CV}). \quad (2)$$

Here $V_{ij}$ is the covariance matrix element of interest, $n_i^{CV}$ is the predicted number of events in the $i$th bin under the nominal (or central-value) GENIE model configuration, and $n_i^k$ is the corresponding event count calculated under an alternate configuration labeled as the $k$th alternate universe. The result is averaged over a total of $N$ alternate universes.

MicroBooNE analyses consider a wide variety of cross section model variations when preparing alternate-universe predictions $n_i^k$ for use with this method. Section V A describes new parameters (and their associated uncertainties) developed by MicroBooNE to address missing degrees of freedom in the reweighting tools released with GENIE v3.0.6. These are supplemented with an external calculation of CCQE model uncertainties related to second-class

TABLE VII. $\chi^2$ for comparisons of GENIE v3.0.6 G18_10a_02_11a and the "MicroBooNE tune" to MiniBooNE flux-averaged CC0$\pi$-like differential cross section data [22], as shown in Fig. 13. Following the information presented in the publication, $\chi^2$ are calculated separately for shape and normalization components, including a reported 10.7% normalization error. Each value is then presented in the table. No correlations between bins were included.

| Prediction | $\chi^2_{\text{shape}}/\text{N}_{\text{bins}}$ | $\chi^2_{\text{norm}}/\text{N}_{\text{bins}}$ |
|---|---|---|
| GENIE v3.0.6 G18_10a_02_11a | 700.14/137 | 7.60/1 |
| "MicroBooNE tune" | 323.87/137 | 1.39/1 |

currents as described in Sec. V B. A full inventory of systematic uncertainties on the GENIE-based cross section model is then documented in Sec. V D and the Appendix.

### A. Additional parameters developed for MicroBooNE interaction uncertainty evaluation

While current MicroBooNE analyses adopt the recommended GENIE v3.0.6 parameter uncertainties in most cases, several new parameters were developed to assess additional uncertainties beyond the default set. Three new parameters (RPA_CCQE, Normccmec, and XSecShape_CCMEC) were already discussed in the context of the tune to T2K CC0$\pi$ data presented in the previous sections. The following paragraphs describe the remaining new parameters which are used for systematic uncertainty evaluation but were excluded from the fit to external data.

Coulomb_CCQE.—The Valencia CCQE model accounts for the Coulomb interaction between the residual nucleus and the outgoing lepton using a procedure similar to the modified effective momentum approximation proposed by Engel [59]. This involves the use of an effective value $k_{\text{eff}}$ of the outgoing lepton momentum computed via

$$E_{\text{eff}} = E - V_C(r) \qquad k_{\text{eff}} = \sqrt{E_{\text{eff}}^2 - m^2}, \tag{3}$$

where $E$ is the lepton total energy, $m$ is its mass, and $V_C(r)$ is the local nuclear Coulomb potential at the initial radial position $r$ of the struck nucleon. An approximate uncertainty on this correction may be assessed by scaling the value of the nuclear Coulomb potential $V_C(r)$. The Coulomb_CCQE parameter applies this scaling with a recommended fractional uncertainty of $\pm 30\%$. The impact of the Coulomb corrections at neutrino energies relevant for MicroBooNE is typically small.

DecayAngMEC.—At present, all 2p2h models implemented in GENIE are inclusive, i.e., they predict the kinematics of the outgoing lepton only [13]. A two-nucleon hadronic final state is obtained in the simulation by recourse to a rough approximation called the nucleon cluster model [50]. Under this approach, the leptonic 4-momentum transfer is imparted to a pair of two nucleons sampled independently from the nuclear ground state distribution and treated as a single object. A decay of the final-state pair is then simulated to produce two outgoing nucleons. In the default GENIE treatment of this decay, the angular distribution is isotropic in the rest frame of the pair. The DecayAngMEC parameter adjusts this behavior. A parameter value of 0 corresponds to the default isotropic distribution, while a value of 1 yields an angular dependence proportional to $\cos^2\theta$, where the polar angle $\theta$ is measured with respect to the 3-momentum transfer $\mathbf{q}$. Due to the lack of theoretical guidance for the alternate angular distribution, this specific form was chosen as a significant deviation from isotropy which is invariant under exchange of the two nucleons. Intermediate parameter values on the interval [0, 1] linearly interpolate between the two distributions. An uncertainty corresponding to the full difference between DecayAngMEC values of 0 and 1 is adopted.

FracPN_CCMEC.—Charged-current 2p2h interactions may occur with an initial pair of nucleons that share the same third component of isospin ($nn$ for neutrinos, $pp$ for antineutrinos) or that differ ($pn$). The FracPN_CCMEC parameter adjusts the fraction of these events involving an initial $pn$ pair relative to the default prediction of the Valencia CC2p2h model. A fractional uncertainty of $\pm 20\%$ is adopted subject to the constraint that the $pn$ fraction must lie on the interval [0, 1].

FracDelta_CCMEC.—In contrast to other theoretical treatments of CC2p2h interactions, the Valencia calculation predicts two distinct peaks in the joint distribution of energy and momentum transfer (see the top panel of Fig. 5). These arise from two classes of Feynman diagrams, one of which involves an internal $\Delta$ line while the other does not. The FracDelta_CCMEC parameter adjusts the relative strength of these two contributions to the CC2p2h cross section. An uncertainty of $\pm 30\%$ on the nominal fraction of CC2p2h interactions that proceed via an internal $\Delta$ is assessed, subject to the constraint that the fraction remains within the interval [0, 1].

Although changes to this parameter were expected to leave the total CC2p2h event rate unchanged, numerical limitations were found that lead to an underprediction of CC2p2h events when the model had fewer relative events with an internal $\Delta$. These limitations involve occasional very large event weights and inconsistencies in the GENIE implementation of the cross sections themselves, e.g., the internal $\Delta$ contribution sometimes exceeds the total cross section. The main impact of these issues on MicroBooNE analyses is expected to be a small overestimation of the systematic uncertainty on the normalization of CC2p2h events.

ThetaDelta2NRad.—An enhanced rate of neutrino-induced production of single photons is a proposed explanation for the anomalous excess of electron-like low-energy events seen by MiniBooNE [60]. Radiative decays of $\Delta$ baryons ($\Delta \to N + \gamma$) are a major source of single photons at MicroBooNE energies and are thus of particular interest. In addition to the existing GENIE uncertainty on the branching ratio for radiative $\Delta$ decay, the new ThetaDelta2NRad parameter is used to assess an uncertainty on the angular distribution for this process. The implementation is similar to the one for the parameter (DecayAngMEC) describing the two-nucleon angular distribution in 2p2h events: a ThetaDelta2NRad value of 0 corresponds to isotropic decays, while a value of 1 yields an angular distribution proportional to $\cos^2\theta$. An uncertainty calculated by taking the full difference between these two extremes is adopted.

NormCCCOH and NormNCCOH.—The event reweighting tools distributed with GENIE v3.0.6 allow for variations

of two parameters in the coherent pion production (COH) cross section: the axial mass (MACOHPI) and the effective nuclear radius (R0COHpi). However, technical limitations in the implementation of the Berger-Sehgal COH model used in G18_10a_02_11a lead to incompatibility with those weight calculators. New parameters which apply a constant scale factor to the CC (NormCCCOH) and NC (NormNCCOH) coherent pion production cross section are adopted instead, each with a $\pm 100\%$ uncertainty.

NormNCMEC.—A similar normalization-only uncertainty of $\pm 100\%$ is assessed on the GENIE empirical model of the NC2p2h cross section.

### B. Second-class current form factors

Violations of charge conjugation or time-reversal symmetry in quasielastic neutrino-nucleon scattering can give rise to new terms in the differential cross section proportional to the second-class current (SCC) form factors $F_V^3$ and $F_A^3$. While the size of the SCC component of the CCQE cross section is limited by measurements of beta decay and related processes, a nonvanishing contribution can lead to noticeable differences in the predicted cross sections for $\nu_e$ and $\nu_\mu$ [61]. Separate systematic uncertainties on the possible contributions of the $F_V^3$ and $F_A^3$ terms in the CCQE cross section are assessed for MicroBooNE analyses via a dedicated weight calculator implemented within the LArSoft software framework [62]. Event weights are evaluated based on the ratio of a CCQE differential cross section calculated using the NEUT [63] neutrino event generator (which includes the SCC form factors) and a similar one calculated with GENIE (which does not). Possible SCC effects for interaction modes other than CCQE are neglected.

### C. Final-state interaction reweighting

The empirical model used in GENIE v3.0.6 G18_10a_02_11a for hadronic final-state interactions is called hA2018 and represents an updated version of the historical default treatment hA used in GENIE v2 [32,64]. An effective cascade approach is employed: each hadron emerging from the primary neutrino interaction vertex may rescatter a maximum of one time inside the nucleus, and the specific reinteraction mode (charge exchange, inelastic, etc.) is sampled using ratios of energy- and $A$-dependent cross sections. The hA FSI models are specifically designed to allow for straightforward uncertainty quantification via reweighting. A key feature of the reweighting strategy is the unitarity constraint. Each change is balanced by changes in other channels to make the overall fraction of events affected by FSI constant. Thus, inclusive event distributions (i.e., those that are not sensitive to final hadron multiplicities and kinematics) are expected to be invariant under FSI model variations [65].

Internal validations of the "MicroBooNE tune" revealed some minor inconsistencies in the hA2018 reweighting tools included with GENIE v3.0.6. These lead to violations of the aforementioned unitarity constraint and thus to potentially inaccurate model uncertainties. The specific issues identified in the weight calculators are (1) the elastic scattering reinteraction mode was removed from the FSI model in the hA $\rightarrow$ hA2018 update, but this change is not fully applied in GENIE reweight; (2) the model parameters and hadron starting positions used to calculate mean free paths in reweight are not completely identical to those used during event generation; and (3) the mass number ($A$) and proton number ($Z$) of the nucleus are not updated to account for prior knockout when reweighting events with multiple primary hadrons.Studies performed by all current MicroBooNE low-energy excess analyses indicate that these problems have a negligible impact on the final results. As with all the other additions covered in this section, this minor inconsistency is fixed in GENIE v3.2.0.

### D. Systematics budget

Table VIII summarizes the ways in which the neutrino interaction model and uncertainties used by MicroBooNE analyses differ from the default GENIE v3.0.6 G18_10a_02_11a configuration. These differences fall into two categories: CCQE and CC2p2h parameters that were tuned as described in this article (and therefore have different central values and uncertainties from the default recommendation), and new parameters developed by MicroBooNE for the evaluation of additional model

TABLE VIII. Summary of parameters for which MicroBooNE analyses adopt a different central value and/or uncertainty than recommended in the GENIE v3.0.6 G18_10a_02_11a model set.

| | "MicroBooNE tune" | | |
|---|---|---|---|
| Parameter | Central value | $+1\sigma$ | $-1\sigma$ |
| MaCCQE[a] | 1.10 GeV | +0.1 GeV | −0.1 GeV |
| RPA_CCQE[b] | 85% | +40% | −40% |
| Normccmec | 166% | +50% | −50% |
| XSecShape_CCMEC | Empirical[c] | N/A | Valencia[d] |
| Coulomb_CCQE | Nominal | +30% | −30% |
| DecayAngMEC | Isotropic | Alternative[e] | N/A |
| FracPN_CCMEC | Valencia | +20% | −20% |
| FracDelta_CCMEC | Valencia | +30% | −30% |
| NormNCMEC | Nominal | +100% | −100% |
| ThetaDelta2NRad | Isotropic | Alternative[e] | N/A |
| NormCCCOH | Nominal | +100% | −100% |
| NormNCCOH | Nominal | +100% | −100% |

[a]The GENIE default value for this parameter is $0.961242 \pm 0.03$ GeV.
[b]Variations are not capped at 100%.
[c]Nominal prediction of the GENIE empirical CC2p2h model.
[d]Nominal prediction of the Valencia CC2p2h model.
[e]An angular distribution proportional to $\cos^2\theta$. See the description of this parameter in Sec. V A.

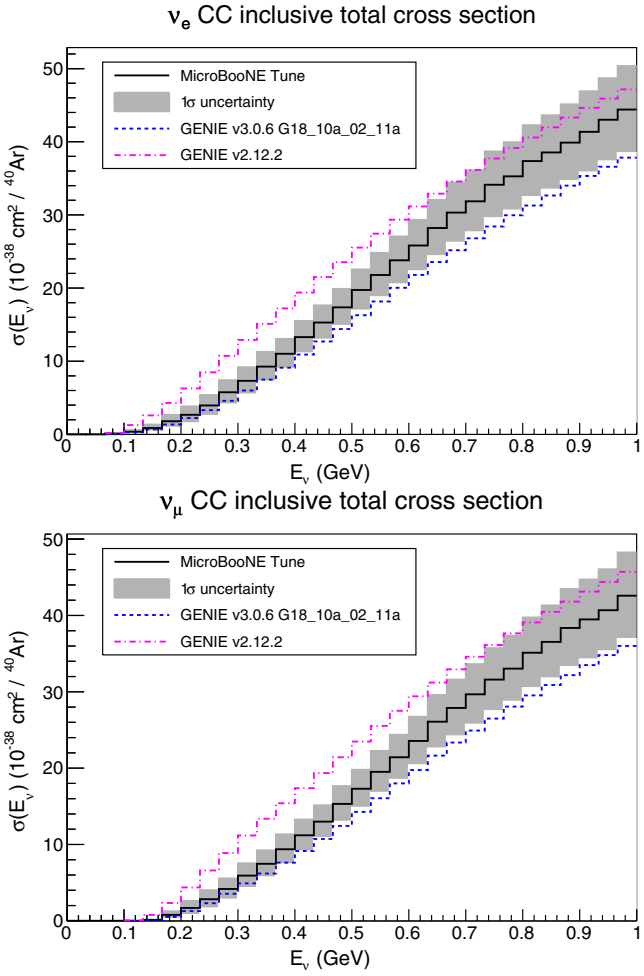


FIG. 14. Predictions from the "MicroBooNE tune" for the CC inclusive total cross section for electron (top) and muon (bottom) neutrino-argon scattering.

uncertainties. For completeness, a full list of parameters for which MicroBooNE analyses adopt the GENIE recommendations unaltered is given in the Appendix.

### E. "MicroBooNE tune" total cross sections with uncertainties

The electron-like LEE searches in MicroBooNE will search specifically for electron neutrino interactions. Therefore it is important to also examine the impact of the "MicroBooNE tune" on the $\nu_e$ CC cross section. The modeling of electron and muon neutrinos in GENIE uses the same underlying model parameters, such that the tune—while derived from fitting to muon-neutrino cross section data—is also applied to the electron neutrino prediction, with uncertainties as previously described. The top (bottom) panel of Fig. 14 shows predictions for the total charged-current cross section for electron (muon) neutrino-argon scattering obtained using the results of our tuning procedure and full treatment of systematic uncertainties. This is plotted as a black line as a function of neutrino energy in the region below 1 GeV where our tune has the largest impact. The gray band indicates the full one-sigma uncertainty for the MicroBooNE standard analysis on the cross section prediction. A comparison is made to the GENIE v3.0.6 G18_10a_02_11a model used as the basis for the tune (dashed blue) and the historical default model from GENIE v2.12.2 (dot-dashed pink).

## VI. SUMMARY AND CONCLUSIONS

This paper introduces a new tune of the GENIE event generator [10] that is suitable for MicroBooNE LEE and cross section analyses. New parameters designed to focus on the most uncertain parts of existing models within GENIE were developed for this purpose.

The T2K inclusive CC0$\pi$ data [16] was the basis for this fit for a variety of reasons. Since there was a strong desire to make this underlying model independent of MicroBooNE data, no internal data was used in the fit. In addition, MiniBooNE data was excluded from the fit to avoid use of a dataset that used the same neutrino beam as MicroBooNE. However, the MiniBooNE CC0$\pi$ data [22] was used as a consistency check.

Initial fits with the full correlated T2K uncertainties resulted in the odd result of a smaller $\chi^2$ and a fit cross section with significantly smaller magnitude than the data. This result was attributed to Peelle's pertinent puzzle [44,48] and only the diagonal uncertainties were used for the fit presented in this work. A number of tests of the robustness of the results were made. Fitting exercises with alternate parameter sets and different starting values gave results very similar to those reported here. Peelle's pertinent puzzle has solutions in the literature [49,66] and one of them [49] was used in an alternate fit. The results are similar to the results reported here, with the alternate fit resulting in parameters within uncertainties of the original fit.

The GENIE G18_10a model set was chosen as the basis for the fit because it provides the best description of data in this kinematic region among available GENIE configurations. It includes the local Fermi gas momentum distribution and the Valencia CCQE [12] and CC2p2h [13] models as implemented in GENIE v3.0.6. As discussed in the text, the implementation in GENIE was somewhat different than what was used in comparisons [11] to MiniBooNE data [22].

Parameters for fitting were chosen according to relevance to the MicroBooNE data and the level of theoretical understanding: the CCQE axial mass, the strength of RPA corrections, the normalization of the CC2p2h cross section, and the shape of the CC2p2h cross section. In particular, CC2p2h and RPA modeling show significant variation among theoretical calculations [1]. Thus, we call these theory-driven fit parameters.

When these parameters were fit to T2K CC0$\pi$ data, both the CCQE and CC2p2h normalizations were increased. The CC2p2h shape parameter had a weak preference for the

one-peak (empirical) shape which is traditional in electron scattering modeling. This sensitivity to CC2p2h shape was not apparent in previous calculations [11]. Although there is a preference for a large RPA contribution as in the Valencia CCQE model [12], the constraint is not strong. The final fit is shown in Fig. 8 with the parameter correlations in Fig. 7.

The interpretation of these fit results should be carefully considered. The fit parameter values only make sense in the context of the modeling parameters and data set used. Given the small number of parameters used, the results indicate directions rather than an actual measurement. The main fit using only diagonal elements of the covariance matrix was presented here for practical reasons. Although it agrees well with a fit using the complete uncertainties, it is not ideal.

The "MicroBooNE tune" leads to a factor-of-two reduction in the T2K data vs simulation chi-squared score when bin-to-bin correlations are neglected ($\chi^2_{\text{diag}}$). However, scores calculated using the more complete definitions of $\chi^2$ listed in Table V show that room remains for future model fitting improvements. In the present scope, performing a fit which describes T2K data optimally is less crucial than obtaining a tuned GENIE model and associated uncertainties which can be applied successfully in MicroBooNE analyses. As seen in Figs. 9–12, the results of this effort provide a noticeably improved match to data most relevant to the LEE search result [3–6]. On the other hand, the ability to describe the MicroBooNE CC inclusive cross section data [55] in Fig. 10 and Table VI is degraded somewhat. The $\chi^2$ is very large in all three cases (untuned GENIE, the "MicroBooNE Ttne," and the alternate fit), perhaps due to the inclusion of additional processes such as pion production which were not included in the fit. In addition, the MicroBooNE CC inclusive cross section measurement was done with an earlier analysis package that relied on GENIE v2 and does not include recent improvements to reconstruction and analysis techniques that were used in the LEE search results [3–6]. More recent CC inclusive cross section data shown in Fig. 11, which include these improvements, typically show better agreement with the "MicroBooNE tune" than with GENIE v3.0.6.

The final fit parameters also produce a better fit to the MiniBooNE data than GENIE v3.0.6. However, it is not a good match to those results. The biggest discrepancies come at the lowest muon momenta.

Nevertheless, the primary goal of producing a parametrization of relevant muon neutrino cross section data has been achieved. This results in an overall improvement for the description of MicroBooNE data as discussed in Sec. IV A. Since the same models are used for muon and electron neutrino CCQE and CC2p2h interactions, this information applies to both flavors and will provide a solid basis for MicroBooNE's searches for physics beyond the Standard Model using electron neutrinos. Since a fit to carbon gives a good description of argon data, the accuracy of the dependence on the nucleus ($A$ dependence) within GENIE for the relevant processes has been demonstrated. This work will also provide the basis for further studies of MicroBooNE cross sections [39,40,55] and other [67] data for heavier targets in the future.

The uncertainty band derived from this work is as important as, and perhaps even more so than, the central-value prediction. The cross section model can be further constrained experimentally through the use of background-enriched and sideband samples, but those procedures rely on a well-motivated quantification of systematic uncertainties in order to work effectively. In particular, this work motivates new uncertainties on parameters for which we previously had no or extremely weak prior uncertainties such as the strength of RPA corrections and the modeling of CC2p2h interactions.

## ACKNOWLEDGMENTS

This document was prepared by the MicroBooNE collaboration using the resources of the Fermi National Accelerator Laboratory (Fermilab), a U.S. Department of Energy, Office of Science, HEP User Facility. Fermilab is managed by Fermi Research Alliance, LLC (FRA), acting under Contract No. DE-AC02-07CH11359. MicroBooNE is supported by the following: the U.S. Department of Energy, Office of Science, Offices of High Energy Physics and Nuclear Physics; the U.S. National Science Foundation; the Swiss National Science Foundation; the Science and Technology Facilities Council (STFC), part of the United Kingdom Research and Innovation; the Royal Society (United Kingdom); and The European Union's Horizon 2020 Marie Sklodowska-Curie Actions. Additional support for the laser calibration system and cosmic ray tagger was provided by the Albert Einstein Center for Fundamental Physics, Bern, Switzerland. We also acknowledge the contributions of technical and scientific staff to the design, construction, and operation of the MicroBooNE detector as well as the contributions of past collaborators to the development of MicroBooNE analyses, without whom this work would not have been possible. We are grateful to the NUISANCE team for extra support for the software tools used in this study. We also thank Stephen Dolan (CERN) for his code implementing the alternate fit in NUISANCE.

## APPENDIX: LIST OF PARAMETERS AND UNCERTAINTIES

Table IX lists all model parameters from GENIE v3.0.6 G18_10a_02_11a for which the central value and uncertainty are adopted unaltered as part of the "MicroBooNE tune" described in this paper. Parameters which have been added or altered by MicroBooNE are listed separately in Table VIII.

TABLE IX. GENIE model parameters used with default settings in the "MicroBooNE tune."

| Parameter | Central value | $+1\sigma$ | $-1\sigma$ |
|---|---|---|---|
| *CCQE form factor parametrization* | | | |
| AxFFCCQEshape | Dipole | $Z$ expansion | N/A |
| VecFFCCQEshape | BBA07 | Dipole | N/A |
| *NC elastic form factors* | | | |
| MaNCEL | 0.961242 GeV | +25% | −25% |
| EtaNCEL | 0.12 | +30% | −30% |
| *RES form factors and decays* | | | |
| MaCCRES | 1.065047 GeV | +20% | −20% |
| MvCCRES | 0.840 GeV | +10% | −10% |
| MaNCRES | 1.120 GeV | +20% | −20% |
| MvNCRES | 0.840 GeV | +10% | −10% |
| RDecBR1gamma | Nominal | +50% | −50% |
| RDecBR1eta | Nominal | +50% | −50% |
| Theta_Delta2Npi | Nominal | Isotropic | N/A |
| *AGKY hadronization model* | | | |
| AGKYxF1pi | −0.385 | +20% | −20% |
| AGKYpT1pi | $1/6.625$ GeV$^2$ | +3% | −3% |
| *Normalization of non-RES final states* | | | |
| NonRESBGvpCC1pi | 0.007713 | +50% | −50% |
| NonRESBGvpCC2pi | 0.787999 | +50% | −50% |
| NonRESBGvnCC1pi | 0.127858 | +50% | −50% |
| NonRESBGvnCC2pi | 2.11523 | +50% | −50% |
| NonRESBGvbarpCC1pi | 0.127858 | +50% | −50% |
| NonRESBGvbarpCC2pi | 2.11523 | +50% | −50% |
| NonRESBGvbarnCC1pi | 0.007713 | +50% | −50% |
| NonRESBGvbarnCC2pi | 0.787999 | +50% | −50% |
| NonRESBGvpNC1pi | 0.1 | +50% | −50% |
| NonRESBGvpNC2pi | 1 | +50% | −50% |
| NonRESBGvnNC1pi | 0.3 | +50% | −50% |
| NonRESBGvnNC2pi | 1 | +50% | −50% |
| NonRESBGvbarpNC1pi | 0.3 | +50% | −50% |
| NonRESBGvbarpNC2pi | 1 | +50% | −50% |
| NonRESBGvbarnNC1pi | 0.1 | +50% | −50% |
| NonRESBGvbarnNC2pi | 1 | +50% | −50% |
| *Bodek-Yang structure functions* | | | |
| AhtBY | 0.538 GeV$^2$ | +25% | −25% |
| BhtBY | 0.305 GeV$^2$ | +25% | −25% |
| CV1uBY | 0.291 GeV$^2$ | +30% | −30% |
| CV2uBY | 0.189 GeV$^2$ | +40% | −40% |
| *Final-state interactions* | | | |
| MFP_pi | hA2018 | +20% | −20% |
| MFP_N | hA2018 | +20% | −20% |
| FrCEx_pi | hA2018 | +50% | −50% |
| FrInel_pi | hA2018 | +40% | −40% |
| FrAbs_pi | hA2018 | +30% | −30% |
| FrPiProd_pi | hA2018 | +20% | −20% |
| FrCEx_N | hA2018 | +50% | −50% |
| FrInel_N | hA2018 | +40% | −40% |
| FrAbs_N | hA2018 | +20% | −20% |
| FrPiProd_N | hA2018 | +20% | −20% |

[1] L. Alvarez-Ruso *et al.* (NuSTEC Collaboration), NuSTEC White Paper: Status and challenges of neutrino–nucleus scattering, Prog. Part. Nucl. Phys. **100**, 1 (2018).

[2] R. Acciarri *et al.* (MicroBooNE Collaboration), Design and construction of the MicroBooNE detector, J. Instrum. **12**, P02017 (2017).

[3] P. Abratenko *et al.* (MicroBooNE Collaboration), Search for an excess of electron neutrino interactions in MicroBooNE using multiple final state topologies, arXiv:2110.14054.

[4] P. Abratenko *et al.* (MicroBooNE Collaboration), Search for an anomalous excess of charged-current $\nu_e$ interactions without pions in the final state with the MicroBooNE experiment, arXiv:2110.14065.

[5] P. Abratenko *et al.* (MicroBooNE Collaboration), Search for an anomalous excess of charged-current quasi-elastic $\nu_e$ interactions with the MicroBooNE experiment using Deep-Learning-based reconstruction, arXiv:2110.14080.

[6] P. Abratenko *et al.* (MicroBooNE Collaboration), Search for an anomalous excess of inclusive charged-current $\nu_e$ interactions in the MicroBooNE experiment using Wire-Cell reconstruction, arXiv:2110.13978.

[7] P. Abratenko *et al.* (MicroBooNE Collaboration), Search for neutrino-induced neutral current $\Delta$ radiative decay in MicroBooNE and a first test of the MiniBooNE low energy excess under a single-photon hypothesis, arXiv:2110.00409.

[8] G. Cheng *et al.* (MiniBooNE and SciBooNE Collaborations), Dual baseline search for muon antineutrino disappearance at $0.1\ \mathrm{eV}^2 < \Delta m^2 < 100\ \mathrm{eV}^2$, Phys. Rev. D **86**, 052009 (2012).

[9] A. A. Aguilar-Arevalo *et al.* (MiniBooNE Collaboration), Neutrino flux prediction at MiniBooNE, Phys. Rev. D **79**, 072002 (2009).

[10] C. Andreopoulos *et al.* (GENIE Collaboration), The GENIE neutrino Monte Carlo Generator, Nucl. Instrum. Methods Phys. Res., Sect. A **614**, 87 (2010).

[11] J. Nieves, I. Ruiz Simo, and M. J. Vicente Vacas, The nucleon axial mass and the MiniBooNE quasielastic neutrino-nucleus scattering problem, Phys. Lett. B **707**, 72 (2012).

[12] J. Nieves, J. E. Amaro, and M. Valverde, Inclusive quasi-elastic neutrino reactions, Phys. Rev. C **70**, 055503 (2004); **72**, 019902(E) (2005).

[13] R. Gran, J. Nieves, F. Sanchez, and M. J. Vicente Vacas, Neutrino-nucleus quasi-elastic and 2p2h interactions up to 10 GeV, Phys. Rev. D **88**, 113007 (2013).

[14] A. Bodek and J. L. Ritchie, Fermi motion effects in deep inelastic lepton scattering from nuclear targets, Phys. Rev. D **23**, 1070 (1981).

[15] V. R. Pandharipande and S. C. Pieper, Nuclear transparency to intermediate-energy nucleons from (e, e'p) reactions, Phys. Rev. C **45**, 791 (1992).

[16] K. Abe *et al.* (T2K Collaboration), Measurement of double-differential muon neutrino charged-current interactions on $C_8H_8$ without pions in the final state using the T2K off-axis beam, Phys. Rev. D **93**, 112012 (2016).

[17] K. Abe *et al.* (T2K Collaboration), First measurement of the $\nu_\mu$ charged-current cross section on a water target without pions in the final state, Phys. Rev. D **97**, 012001 (2018).

[18] K. Abe *et al.* (T2K Collaboration), Characterization of nuclear effects in muon-neutrino scattering on hydrocarbon with a measurement of final-state kinematics and correlations in charged-current pionless interactions at T2K, Phys. Rev. D **98**, 032003 (2018).

[19] K. Abe *et al.* (T2K Collaboration), First combined measurement of the muon neutrino and antineutrino charged-current cross section without pions in the final state at t2k, Phys. Rev. D **101**, 112001 (2020).

[20] K. Abe *et al.* (T2K Collaboration), Simultaneous measurement of the muon neutrino charged-current cross section on oxygen and carbon without pions in the final state at t2k, Phys. Rev. D **101**, 112004 (2020).

[21] A. A. Aguilar-Arevalo *et al.* (MiniBooNE Collaboration), Measurement of Muon Neutrino Quasi-Elastic Scattering on Carbon, Phys. Rev. Lett. **100**, 032301 (2008).

[22] A. Aguilar-Arevalo *et al.* (MiniBooNE Collaboration), First measurement of the muon neutrino charged current quasielastic double differential cross section, Phys. Rev. D **81**, 092005 (2010).

[23] M. F. Carneiro *et al.* (The MINER$\nu$A Collaboration), High-Statistics Measurement of Neutrino Quasielasticlike Scattering at 6 gev on a Hydrocarbon Target, Phys. Rev. Lett. **124**, 121801 (2020).

[24] T. Cai *et al.* (The MINER$\nu$A Collaboration), Nucleon binding energy and transverse momentum imbalance in neutrino-nucleus reactions, Phys. Rev. D **101**, 092001 (2020).

[25] D. Ruterbories *et al.* (MINERvA Collaboration), Measurement of quasielastic-like neutrino scattering at $\langle E_\nu \rangle \sim 3.5$ GeV on a hydrocarbon target, Phys. Rev. D **99**, 012004 (2019).

[26] X.-G. Lu *et al.* (MINERvA Collaboration), Measurement of Final-State Correlations in Neutrino Muon-Proton Mesonless Production on Hydrocarbon at $\langle E_\nu \rangle = 3$ GeV, Phys. Rev. Lett. **121**, 022504 (2018).

[27] M. Betancourt *et al.* (MINERvA Collaboration), Direct Measurement of Nuclear Dependence of Charged Current Quasielasticlike Neutrino Interactions Using Minerva, Phys. Rev. Lett. **119**, 082001 (2017).

[28] T. Walton *et al.* (MINERvA Collaboration), Measurement of muon plus proton final states in $\nu_\mu$ interactions on hydrocarbon at $\mathrm{e}_\nu = 4.2$ GeV, Phys. Rev. D **91**, 071301 (2015).

[29] G. A. Fiorentini *et al.* (MINERvA Collaboration), Measurement of Muon Neutrino Quasielastic Scattering on a Hydrocarbon Target at $E_\nu \sim 3.5$ GeV, Phys. Rev. Lett. **111**, 022502 (2013).

[30] O. Palamara (ArgoNeuT Collaboration), Exclusive muon neutrino charged current pion-less topologies. Argoneut results and future prospects in lar tpc detectors, *Proceedings of the 10th International Workshop on Neutrino-Nucleus Interactions in Few-GeV Region (NuInt15)* (Physical Society of Japan, Tokyo, Japan, 2016), p. 010017.

[31] R. Acciarri *et al.* (ArgoNeuT Collaboration), Detection of back-to-back proton pairs in charged-current neutrino interactions with the ArgoNeuT detector in the NuMI low energy beam line, Phys. Rev. D **90**, 012008 (2014).

[32] L. Alvarez-Ruso *et al.* (GENIE Collaboration), Recent highlights from GENIE v3, Eur. Phys. J. Special Topics **230**, 4449 (2021).

[33] K. M. Graczyk and J. T. Sobczyk, Lepton mass effects in weak charged current single pion production, Phys. Rev. D **77**, 053003 (2008).

[34] C. Berger and L. M. Sehgal, Lepton mass effects in single pion production by neutrinos, Phys. Rev. D **76**, 113004 (2007); **77**, 059901(E) (2008).

[35] K. S. Kuzmin, V. V. Lyubushkin, and V. A. Naumov, Lepton polarization in neutrino nucleon interactions, Mod. Phys. Lett. A **19**, 2815 (2004).

[36] J. A. Nowak (MiniBooNE Collaboration), Four momentum transfer discrepancy in the charged current $\pi^+$ production in the MiniBooNE: Data vs. Theory, AIP Conf. Proc. **1189**, 243 (2009).

[37] J. Tena-Vidal *et al.* (GENIE Collaboration), Neutrino-nucleon cross-section model tuning in GENIE v3, Phys. Rev. D **104**, 072009 (2021).

[38] P. Abratenko *et al.* (MicroBooNE Collaboration), First Measurement of Inclusive Muon Neutrino Charged Current Differential Cross Sections on Argon at $E_\nu \sim 0.8$ GeV with the MicroBooNE Detector, Phys. Rev. Lett. **123**, 131801 (2019).

[39] P. Abratenko *et al.* (MicroBooNE Collaboration), First Measurement of Differential Charged Current Quasielastic-like $\nu_\mu$-Argon Scattering Cross Sections with the MicroBooNE Detector, Phys. Rev. Lett. **125**, 201803 (2020).

[40] P. Abratenko *et al.* (MicroBooNE Collaboration), Measurement of differential cross sections for $\nu_\mu$-Ar charged-current interactions with protons and no pions in the final state with the MicroBooNE detector, Phys. Rev. D **102**, 112013 (2020).

[41] P. Abratenko *et al.* (MicroBooNE Collaboration), Measurement of the flux-averaged inclusive charged-current electron neutrino and antineutrino cross section on argon using the NuMI beam and the MicroBooNE detector Phys. Rev. D **104**, 052002 (2021).

[42] R. González-Jiménez, M. B. Barbaro, J. A. Caballero, T. W. Donnelly, N. Jachowicz, G. D. Megias, K. Niewczas, A. Nikolakopoulos, and J. M. Udías, Constraints in modeling the quasielastic response in inclusive lepton-nucleus scattering, Phys. Rev. C **101**, 015503 (2020).

[43] P. A. Rodrigues *et al.* (MINERvA Collaboration), Identification of Nuclear Effects in Neutrino-Carbon Interactions at Low Three-Momentum Transfer, Phys. Rev. Lett. **116**, 071802 (2016); **121**, 209902(A) (2018).

[44] T. Bonus, J. T. Sobczyk, M. Siemaszko, and C. Juszczak, Data based two-body current contribution to neutrino-nucleus cross section, Phys. Rev. C **102**, 015502 (2020).

[45] P. Stowell, C. Wret, C. Wilkinson, L. Pickering, S. Cartwright, Y. Hayato, K. Mahn, K. McFarland, J. Sobczyk, R. Terri, L. Thompson, M. Wascko, and Y. Uchida, NUISANCE: A neutrino cross-section generator tuning and comparison framework, J. Instrum. **12**, P01016 (2017).

[46] M. Betancourt *et al.*, Comparisons and challenges of modern neutrino scattering experiments (TENSIONS2016 report), Phys. Rep. **773–774**, 1 (2018).

[47] P. Stowell *et al.* (MINERvA Collaboration), Tuning the GENIE pion production model with MINER$\nu$A data, Phys. Rev. D **100**, 072005 (2019).

[48] K. Hanson, T. Kawano, and P. Talou, Probabilistic interpretation of Peelle's Pertinent Puzzle and its resolution, AIP Conf. Proc. **769**, 304 (2005).

[49] L. Koch, Robust test statistics for data sets with missing correlation information, Phys. Rev. D **103**, 113008 (2021); J. Chakrani, M. Buizza Avanzini, and S. Dolan, Parametrising CCQE uncertainties in the spectral function model for neutrino oscillation analyses, arXiv:2202.03219.

[50] T. Katori, Meson exchange current (MEC) models in neutrino interaction generators, AIP Conf. Proc. **1663**, 030001 (2015).

[51] J. Amaro, M. Barbaro, J. Caballero, R. González-Jiménez, G. Megias, and I. Ruiz Simo, Electron- versus neutrino-nucleus scattering, J. Phys. G **47**, 124001 (2020).

[52] P. Abratenko *et al.*, First measurement of inclusive electron-neutrino and antineutrino charged current differential cross sections in charged lepton energy on argon in MicroBooNE, arXiv:2109.06832.

[53] P. Abratenko *et al.* (MicroBooNE Collaboration), First measurement of energy-dependent inclusive muon neutrino charged-current cross sections on argon with the MicroBooNE detector, arXiv:2110.14023.

[54] P. Abratenko *et al.* (MicroBooNE Collaboration), High-performance generic neutrino detection in a LArTPC near the earth's surface with the MicroBooNE detector, arXiv:2012.07928.

[55] P. Abratenko *et al.* (MicroBooNE Collaboration), First Measurement of Inclusive Muon Neutrino Charged Current Differential Cross Sections on Argon at $E_\nu \sim 0.8$ GeV with the MicroBooNE Detector, Phys. Rev. Lett. **123**, 131801 (2019).

[56] X. Ji, W. Gu, X. Qian, H. Wei, and C. Zhang, Combined Neyman–Pearson chi-square: An improved approximation to the Poisson-likelihood chi-square, Nucl. Instrum. Methods Phys. Res., Sect. A **961**, 163677 (2020).

[57] E. J. Moniz, I. Sick, R. R. Whitney, J. R. Ficenec, R. D. Kephart, and W. P. Trower, Nuclear Fermi Momenta from Quasielastic Electron Scattering, Phys. Rev. Lett. **26**, 445 (1971).

[58] GENIE Reweight, https://github.com/GENIE-MC/Reweight.

[59] J. Engel, Approximate treatment of lepton distortion in charged current neutrino scattering from nuclei, Phys. Rev. C **57**, 2004 (1998).

[60] A. A. Aguilar-Arevalo *et al.* (MiniBooNE Collaboration), Significant Excess of Electronlike Events in the MiniBooNE Short-Baseline Neutrino Experiment, Phys. Rev. Lett. **121**, 221801 (2018).

[61] M. Day and K. S. McFarland, Differences in quasielastic cross sections of muon and electron neutrinos, Phys. Rev. D **86**, 053003 (2012).

[62] E. Snider and G. Petrillo, LArSoft: Toolkit for simulation, reconstruction and analysis of liquid argon TPC neutrino detectors, J. Phys. Conf. Ser. **898**, 042057 (2017).

[63] Y. Hayato, A neutrino interaction simulation program library NEUT, Acta Phys. Pol. B **40**, 2477 (2009).

[64] S. Dytman, Y. Hayato, R. Raboanary, J. T. Sobczyk, J. Tena-Vidal, and N. Vololoniaina, Comparison of validation

methods of simulations for final state interactions in hadron production experiments, Phys. Rev. D **104**, 053006 (2021).
[65] C. Andreopoulos, C. Barry, S. Dytman, H. Gallagher, T. Golan, R. Hatcher, G. Perdue, and J. Yarba, The GENIE neutrino Monte Carlo generator: Physics and user manual, arXiv:1510.05494.
[66] V. G. Pronyaev *et al.*, Status of the international neutron cross-section standards file, AIP Conf. Proc. **769**, 808 (2005).
[67] R. Acciarri *et al.* (ArgoNeuT Collaboration), First measurement of electron neutrino scattering cross section on argon, Phys. Rev. D **102**, 011101 (2020).